Applied Energy 409 (2026) 127420

Contents lists available at ScienceDirect

Applied Energy

journal homepage: www.elsevier.com/locate/apenergy

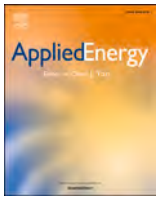

Decarbonization pathways of Hard-to-Abate sectors through hydrogen blending solutions☆

S. Mazzoni *, M. Vellini, M. Gambini

University of Roma Tor Vergata, Italy

HIGHLIGHTS

- Hard-to-Abate sector decarbonisation via structured modelling of demand & supply
- Introduction of H2 blending maps for accounting emissions factors and OPEX
- H2 in Hard-to-Abate allows for near-future decarbonization goal achievements.
- Up to 80% CO2 reduction observed when high-temperature heat is generated via H2.

ARTICLE INFO

Keywords:
Fuel diversification
H2 economy
Decarbonization
Industrial process
Hard-to-Abate

ABSTRACT

Following up on European Regulatory plans towards carbon neutrality targets by exploiting cost-effective, reliable and easy-to-implement solutions based on hydrogen penetration in the Hard-to-Abate sectors are a challenge. Under this umbrella, the authors proposed a methodological approach to model the demand and supply of HTA sector needs (e.g. electricity, heat), integrated with proprietary databases of H2-specific production costs and related CO_2 emission factors, and of HTA sectors (e.g. refinery, paper production, glass & steel manufacturing) specific consumptions (electricity, heat) and emissions per production unit. The authors presented an H2-CH4 blending model capable of assessing blended fuel CO_2 emission factors and OPEX through maps. The first map shows that achieving a specific decarbonization target, as an example, 20% in respect of the current configuration, requires up to 70% blending of blue H2 (80 kg CO_2/MWh emission factor) or only 50% blending of green H2 (near-zero CO_2 emissions). The second map incorporates LCOH and Carbon Tax to evaluate economic feasibility. In a case study with CH4 priced at 70 EUR/MWh and CO_2 Tax of 100 EUR/ton, green H2 remains costlier, while blue H2 blending leads to a slight OPEX reduction of 2 EUR/MWh, since Carbon Tax is applied. Thanks to these maps, a sensitivity analysis varying H2 blending fraction with CH4 has been performed for five HTA sectors, highlighting CO_2 emissions reduction potential, up to 70% in the sectors with larger heat demands, such as Oil&Gas, and evaluating OPEX in respect to the reference scenario, showing that at the current CO_2 Tax of almost 100 EUR/ton and for the actual LCOH the decarbonisation economic viability would require the support of regulation and environmental policies implementation.

1. Introduction

Globally worldwide, governmental policies on climate change are aligned on the need for a collective effort to phase out fossil fuels progressively ("Transition away") while simultaneously seeking and investing in forms of carbon-neutral energy sources, primarily supporting the development of renewable ones (RES) [1]. Indeed, recently, at COP28 in Dubai, countries that historically based their core business on fossil fuels trading acknowledged the importance of switching to alternative energy carriers. [1,2]

Accordingly, it has been proven over the last decades that to tackle the Net-Zero Challenges successfully, a synergetic approach ranging from the RES penetration, the holistic integration of E-Fuels in the Circular Economy [3] context and arriving at innovative solutions based on advanced R&D projects for reducing costs and increasing effectiveness of equipments addressed to CCS & CCU is required. At the same time, to

☆ This article is part of a Special issue entitled: 'Nexus of EEE' published in Applied Energy.

* Corresponding author.
E-mail addresses: stefano.mazzoni@uniroma2.it (S. Mazzoni), vellini@ing.uniroma2.it (M. Vellini), gambini@ing.uniroma2.it (M. Gambini).

https://doi.org/10.1016/j.apenergy.2026.127420
Received 30 December 2024; Received in revised form 6 December 2025; Accepted 15 January 2026
Available online 29 January 2026

establish a priority list of actions to be taken, it is essential to look at the carbon intensity related to different processes and the easy-to-implement strategy to reduce CO_2 emissions in the near term while moving towards 2050 goals.

Among energy-intensive sectors, those requiring necessary actions correspond to heavy industries such as Cement, Iron & Steel and Glass Manufacturing, Oil&Gas, and Paper production, where requirements of high temperature on one side and high energy density on the other make their decarbonization a challenge [4]. Nevertheless, decarbonisation strategies are difficult to implement in other market segments, such as Aviation and Shipping [5], where stringent operating conditions occur [6,7], and where integration of power-to-fuel solutions based on Green H2 production from RES is gaining traction lately, as widely discussed by [8].These sectors fall under the definition of the Hard-to-Abate (HTA) ones. HTA sectors contribute significantly to global CO_2 emissions, and their decarbonization potential varies widely depending on the technologies and strategies applied, and it is strictly connected with the specific location and application.

Indeed, the Iron and Steel HTA sector accounts for approximately 7% of global CO_2 emissions [4], with blast furnace-basic oxygen furnace (BF-BOF) processes emitting nearly 2 t of CO_2 per tonne of steel. Promising solutions that implement advanced technologies like hydrogen-based direct reduction and electric arc furnaces offer up to 90% emission reductions [9], while carbon capture and storage (CCS) combined with existing methods can achieve 86% savings, with the drawback of a relatively relevant increase in the energy use by 17% [10]. Some of early stage alternatives, such as scaling up iron ore electrolysis and hydrogen-based plasma reduction still see issues related to the low TRL, and indeed is limited by deep sensitivity to feed variations, requiring more R&D steps in obtaining inert anodes and electrode designs [11,12]. In [13], the authors have performed a deep state the art investigation on the potetial alternatives for steel decarbonization, having identified viable option, with both economic and technical potential in H2 integration. In addition, it has been proven that H2 blending integration in the sector, especially when CCS solutions are not available, can lead up to 25% CO_2 emission reduction [14].

Looking at the HTA Chemical sectors, they are responsible for up to 14% of industrial emissions since key products like ammonia and high-value chemicals (e.g., ethylene) are highly emissions-intensive [4,15]. Among the existing solutions, for decarbonizing the chemical sector, electric steam crackers and CCS can cut emissions by 90–100% for high-value chemicals, requiring anyway a significant energy consumption that drastically reduces the production cycle efficiency, requiring still more R&D activities for better integrating the solutions with the existing processes. Alternatively, the integration of green H_2 for ammonia synthesis can achieve 100% decarbonisation, but also in this case a significant energy cost increase is observed [16,17].

The construction material market segment, including the cement and lime production, contributes due to the high energy-intensive processes to up to 40–50% of the overall emissions of the construction HTA sector [18–20]. Presently, CCS technologies (e.g. advanced amines) can capture up to 95% of emissions, but the solution's maturity is still in the (6–8) TRL [21–23]. Accordingly, alternative materials, such as magnesium-based cement, offer up margin to achieve up to 60% CO_2 emissions reduction [13]. Concurrently, among innovative decarbonization technologies the integration of low-capacity plasma torches is a promising option, but still the not adequate alkalinity [24,25] requires the need for testing and integration of new reinforcements like polymer composites. Looking at up-stream decarbonization solutions, like fuel switching to biomass or green H2 can cut up to 25–40% of the CO_2 emissions, at increase cost of production. In [26], the authors demonstrate that by integrating H2 into oxy-combustion, despite the loss in the overall efficiency, a saving up to 27% in the overall CO_2 emissions was observed.

The CO_2 emissions in the aluminium value chain are broken down 62–67% of the total from electricity usage in the electrolysis process, 13–16% comes from thermal energy consumption, 9–12% from process-related emissions, and the rest is linked to the use of ancillary raw materials [4]. Some of the solutions for decarbonising aluminium production account for the recycling aluminium scrap providing the highest reduction potential (95%), while inert anodes and low-carbon electricity can cut emissions significantly, too [27].

Another energy-intensive HTA sector is glass production. The high-temperature furnaces dominate emissions in glass production, with almost up to 70–80% [28,29] of the overall energy consumption of the glass industry, and when based on fossil fuels, also for the corresponding CO_2 emissions. Among the solutions available in the literature for accomplishing the decarbonisation targets, electrification of low and medium-temperature processes and E-fuel switching can reduce up to 80% of emissions [30]. At the same time, plasma melting and hybrid furnaces offer significant potential but with relatively low (4–6) TRL. It should be highlighted that glass production via plasma melting is constrained by scalability and expensive argon gas. A recent scientific paper proposed a relevant analysis of the green H2 integration in the hollow glass manufacturing sector, by up to 20% CH4-H2 blending ratio, demonstrating up to 960 CO_2 ton per year of savings, when dealing with a plant capacity of almost 90 kton per year of glass production [31].

Oil & Gas sector and refineries are emission-intensive, with 51–63% of emissions originating from furnaces used for process heat, 21% from hydrogen production (typically via steam methane reforming), 10% from CHP and boiler fuel use, and 9% from catalytic cracking [32]. Recent studies forecast potential achievements in up to 63% CO_2 emissions reduction, including CCS [33,34], and among the innovative alternatives refining processes like cold cracking are still limited by material handling inefficiencies, not allowing large-scale implementation [33]. Among the solutions that can be implemented in the short term, switching furnaces and H_2 production to a low-carbon alternative, desirably by green H_2 or electrification already shown promising results [34].

The ceramics HTA sector faces significant decarbonization challenges due to its reliance on high-temperature processes for firing and drying. The energy-intensive processes occurring in kilns operating at 1000–1300 °C, and producing emissions from fuel combustion (78%) and process chemistry (16%). Decarbonization options in ceramics include electrification of firing and drying processes, which could reduce emissions by up to 50%, even if current (TRLs) remain low (3–5). Fuel switching to hydrogen or biogas offers a similarly significant reduction [4], while novel approaches like microwave or spark plasma sintering present promising but nascent solutions (TRL 1–2) [35].

The results of the analysis of the most up-to-date state of the art of the HTA sectors, ranging from the Iron manufacturing, Oil & Gas, and ceramics sectors, have led to the identification of some barriers in defining a common strategy towards decarbonisation, since each sector is characterised by different energy intensity, by heat demands at different temperature levels, by different water utilisation and by different plant complexity. Furthermore, some of the promising technological solutions proposed by the R&D experts still showcase low-TRL and small pilot demonstrators that are not allowing their implementation in the short term [4].

To speed up and find alternative manners to effectively decarbonise the above-mentioned HTA sectors, the integration of advanced plant configurations, characterised by enhanced energy efficiency measures coupled with fuel diversification, like H2, [36] and heat processes electrification, becomes pivotal for the effective deployment of ready-to-implement decarbonization pathways in HTA sectors. Furthermore, the decarbonization of HTA sectors demands tailored solutions addressing scalability, operational efficiency, and cost, coupled with cross-sector collaboration and innovation, to achieve sustainable progress. Indeed, recent studies focus the attention on the holistic integration of alternative energy carriers such as H2 to supply multiple demands, while ensuring optimal H2 system integration [37].

[38–40] A model for evaluating the blending of H_2 with CH_4, and

understanding both from the emission and cost standpoint, which are the optimal blending ratios, in respect of H2 production technology (green, grey, brown, etc), summarized in Table 1, of the specific application in the HTA sectors, and of the energy system technological limitation has been also presented and discussed.

Accordingly, this work focuses on the heavy industry Hard-to-Abate sectors related to goods manufacturing (iron and steel, cement, glass, paper) as well as the oil and gas sector. Building on these specific applications, the authors propose a general modelling framework that can be readily adapted to assess, from an environmental techno-economic standpoint, the decarbonisation potential of any HTA sector and, more broadly, of smart industrial districts where electricity, heat, cooling and water are concurrently needed [41].

The proposed approach introduce elements of novelties when compared with the existing apporach, since demands and supply are matched holisitcally. Indeed, on the demand side, the authors introduce a unified Energy Consumption Model that consistently represents the electricity and thermal loads of different HTA sectors. The model draws on established datasets from the state of the art [41] as well as on the authors' prior process-level experience [38–40], thereby enabling the construction of a harmonised database of sector-specific energy consumption profiles. On the supply side, the authors develop a Multi-Energy Supply Model that allows for the evaluation of HTA operation of combined heat and power units, fuel and electric boilers, heat pumps and grid exchanges. This formulation, one the basis of previous work [42], enables the simultaneous provision of electricity, heat, cooling and water, and allows a complete allocation of CO_2 emissions and costs across the energy supply mix.

A further contribution of this work is the explicit treatment of hydrogen blending into methane as a decision variable in the optimisation problem. The model links the H_2–CH_4 blending ratio to techno-economic parameters of diverse hydrogen production pathways (green, blue, grey, brown, etc.), as per Table 1, represented through generic cost and emission factors, and incorporates sector-specific

Table 1
Circular table of hydrogen colour classification.

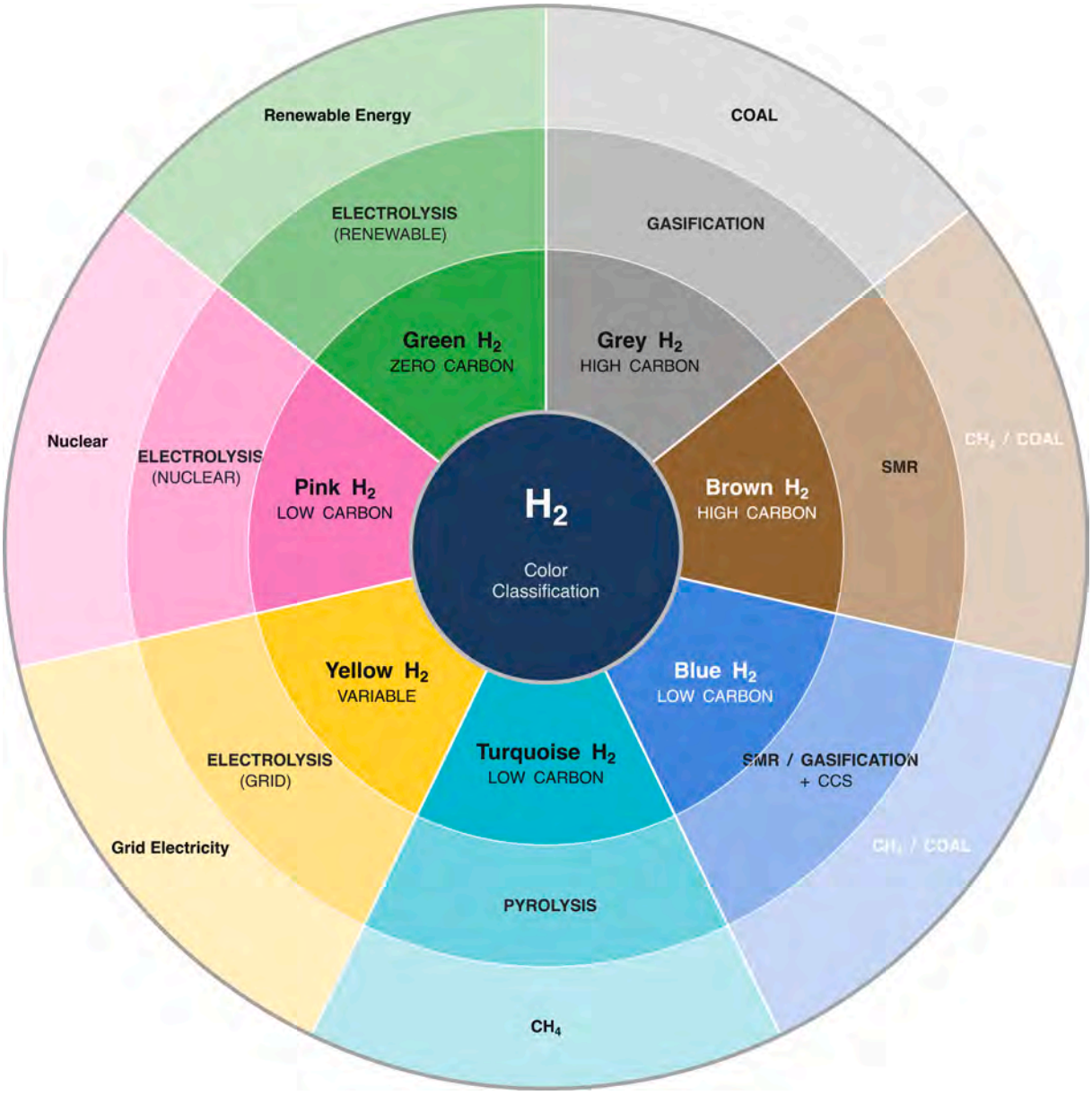

blending limits on the energy system side. In this way, the framework determines, for each HTA sector and for aggregated industrial districts, the optimal hydrogen blending ratio with respect to both emissions and cost. Additionally, a two-dimensional sensitivity analysis is performed by varying the hydrogen emission factor ($kgCO_2$/MWh) and hydrogen cost (€/MWh), thereby identifying the break-even regions where hydrogen blending becomes an effective decarbonisation strategy for HTA process heat.

Compared with previous studies on HTA decarbonisation [41] and multi-energy system integration of hydrogen [41,43], the proposed methodology provides a holistic environmental techno-economic assessment through three principal innovations. First, the authors present a generic and easily customisable HTA Energy Consumption Model capable of representing multiple industrial sectors within a unified formulation, directly linked to sectoral energy-use databases. Second, the authors introduce a multi Energy Supply Model suitable for HTA applications and readily extendable to smart industrial districts requiring simultaneous management of electricity, heat, cooling and water under techno-economic and environmental constraints. Third, the framework incorporates low-carbon energy carriers through an explicit evaluation of the hydrogen–methane blending ratio potential. By linking the multi-energy system to databases of hydrogen production costs and carbon intensities, as well as to the HTA energy consumption profiles, the proposed model quantifies the potential of hydrogen integration to reduce Scope 1 and Scope 2 CO_2 emissions and identifies the most promising technology options and blending ratios that balance decarbonisation performance with cost effectiveness.

In the next section, the proposed methodology is provided, and subsequently, the authors present a section with a holistic system layout, where the matching between k-HTA sectors' electricity and heat demands and Multi-Energy System configuration, equipped with CHP, Boilers (fuel and electric), Heat Pumps and national grid, and H2 blending into CH4, is guaranteed. From the numerical point of view, the authors present a sensitivity analysis related to the impact that H2 emissions factors, expressed in kg CO_2/MWh, and cost, expressed in euro/MWh, have on defining the optimal blending ratio. Also, the authors evaluate the impact of varying the H2 blending ratio (0–100%), when the heat demand of the above-mentioned HTA sectors is generated via blended H2-CH4 fuel.

1.1. Technical background

In the paper, the authors investigate the potential of integrating alternative energy carriers, such as H_2, in the HTA sectors for achieving carbon emissions reduction and evaluating the economic impact of adopting an alternative energy carrier with respect to the typical CH_4. To quantify the environmental techno-economic feasibility of H2 penetration in the HTA sectors, the authors have investigated H2 production technologies and the related costs and emissions, building up a database that includes H2-specific costs, namely LCOH (€/kgH2) and specific emission ($kgCO_2$/kgH2), shown in Table 2. Similarly, the authors have adopted an existing database [38,44], built up by the authors, for accounting for the specific energy consumption, in this case only accounting for Heat (H) and Electricity (E) of each HTA sector. In this paper, the authors implemented in the global model the capabilities of the second database adopting data related to the different HTA sectors yearly production capacity [38], with the scope to evaluate the specific cost (€/Up) and specific emission ($kgCO_2$/Up), per unit of product (Up), as shown in Table 3.

Accordingly, to structure methodically the simulation framework, and thus evaluate the CO_2 emission reduction potential and the related economic evaluation in the HTA sectors via H2 blending within CH4, the authors have investigated from the most up-to-date state of the art, which are costs (CAPEX and OPEX), emission factors, and technical limitations of the different technologies for producing H_2, coupling them with the well-established differentiation of H_2 Colours reported in Table 1, based on scientific publication [45–48] that investigates different H2 production framework. Each H_2 colour indeed is characterized by an H_2 production process (i.e. Gasification, Steam Reforming, Electrolysis), a Primary Energy Source (i.e. fossil fuel, nuclear) and an Energy Vector (i.e. electricity) required for the accomplishment of the H_2 production processes. In the circular table, external circle represents the energy source/carrier, the middle circle the production technology, and the inner circle shows the related H2 colour. Following a well-structured approach, the authors summarised the results of deep research in the scientific literature [46], in the H2 production database, given in Table 2. This database includes a minimum and maximum range for the LCOH ranging between 1.0 and 37.0 €/kgH2 [49,50], and values ranging between 0.0 and 20.0 kg CO_2 /kgH2 the specific CO_2 emissions for kg of H2 and the TRL level related to the market readiness of the proposed production. It is important to remark that for some technologies, such as dark fermentation and H2 production from biomass, the emission factor has been set equal to 0.0 since they are typically considered carbon-neutral technologies [49,50]. Still, the handling of the produced H2and the related shipping/transportation, despite the important improvements in the H2 production and transportation value chain [51], will also add –in the order 0.25–0.50 kg CO_2 /kgH2 [52,53] – a small contribution to the overall CO_2 emissions. It's

Table 2
Summary of hydrogen production methods [45–48].

Source	N	Production method	min LCOH [EUR/kgH2]	MAX LCOH [EUR/kgH2]	min kgCO2/kgH2	MAX kgCO2/kgH2	MATURITY [TRL]
Methane	1	SMR	1.0	2.0	8.0	10.0	8–9
	2	SMR + CCUS	2.0	2.5	2.0	**	8–9
	3	PYROLYSIS	2.0	2.5	4.2	9.1	7–8
Coal	4	GASIFICATION	1.1	1.5	18.0	20.0	8–9
	5	GASIFICATIONS + CCUS	2.0	5.0	3.0	**	8–9
Electricity	6	ELECTROLYSIS BY NUCLEAR	4.0	7.0	0.1	0.3	/
(+ water)	7	ELECTROLYSIS BY ON -SH WIND	4.0	12.0	0	0	/
	8	ELECTROLYSIS BY OFF -SH WIND	4.0	11.0	0	0	/
	9	ELECTROLYSIS BY SOLAR PV	5.0	12.0	0	0	/
	10	ELECTROLYSIS BY GRID	***	***	***	***	/
Biomass	11	PYROLYSIS	1.3	2.5	CO2 NEUTRAL	CO2 NEUTRAL	5–6
	12	GASSIFICATION	1.7	2.8	CO2 NEUTRAL	CO2 NEUTRAL	8–9
	13	DIRECT BIO-PHOTOLYSIS	3.2	26.9	CO2 NEUTRAL	CO2 NEUTRAL	4–6
	14	INDIRECT BIO-PHOTOLYSIS	1.4	/	CO2 NEUTRAL	CO2 NEUTRAL	6–8
	15	DARK FERMENTATION	2.6	26.7	CO2 NEUTRAL	CO2 NEUTRAL	4–6
	16	PHOTO-FERMENTATION	2.8	37.2	CO2 NEUTRAL	CO2 NEUTRAL	4–6

Note: Storage and Transportation costs are not included.
** Depends on CCS ratios.
*** Depends on National Policies and Costs.

Table 3
HTA sectors E & H consumptions, costs and specific emissions for ton of unit production [38–40,44].

HTA sectors	E	H	CO_{2_E}	CO_{2_H}	$EURO_E$	$EURO_H$	CO_{2_H}/CO_{2_E}
	[kWh_E/ton]	[kWh_H/ton]	$kgCO_2$/ton	$kgCO_2$/ton	€ /ton	€ /ton	[−]
Glass	400	200	128	47	110	16	0.4
Oil & gas	80	240	26	56	22	19	2.2
Paper	750	1500	239	350	206	117	1.5
Ceramic	100	100	32	23	28	8	0.7
Iron & steel	680	170	217	40	187	13	0.2

important to note that especially for Low TRL solutions, the proposed LCOH costs, despite the comprehensive literature review carried out by the authors [54], can vary in a wide range with respect to different factors such as feedstock availability, process efficiency, the scale of operation, and technological advancements. Additionally, some of these technologies are still in the research and development stages, and their commercial viability may improve with further innovation and investment.

With similarities to what has been done for the H2 production, the authors, thanks to the experience gained in the field over the last years [38–40,44], and an up-to-date technical background assessment [55], have built up the database of the HTA sectors, For each HTA sector investigated in the paper, the electrical (E) and heat demand (H) for the unit of production, the CO_2 -specific emissions for the unit of production for E, when generated with the national grid, and useful heat H, when generated by CH4, expressed in kg CO_2 /ton, and similarly the specific costs, expressed in €/Ton of production. The ton of production refers to the produced asset from each of the HTA sectors, thus referring to the ton of crude steel, crude oil, glass and so for the other. The value proposed in Table 3 are based on a CH4 cost of 70 €/MWh and a related fuel emission factor of 0.210 kg CO_2 /kWh, on an electricity price of 275 €/MWh, and a related grid emission factor of 0.319 kg CO_2 /kWh, when considering Italian National Grid 2023 data. In the last column the ratio between the CO_2 emissions associated to the electricity and the fuel combustion has been also introduced, in order to understand which are the HTA sectors with more decarbonization potential, in respect of substituting fossil fuels with alternative ones. The development of those DBs allows for a systematic classification of the H2 production technologies and for connecting production technologies to the utilisation in the HTA sectors.

2. Material & methods

The optimal integration of alternative energy sources and energy carriers, preferably with reduced environmental impact, such as renewables or alternative fuels, like H_2, into well-established industrial processes requires a systematic approach to understanding how different HTA sectors demand, in terms of electricity (*E*), cold energy (*C*), heat (*H*) and water (*W*), can be optimally supplied by smart multi-energy systems, where concurrent generation of the required assets takes place [56]. In a broader manner, looking at integrated industrial districts [57], the authors have proposed a modelling approach that allows the aggregation, and the simulation of industrial estates made up of multiple HTA sectors, where the concept of industrial districts can also be accounted for. Indeed, heat recovery processes and waste heat management coupled with district heat & cooling operations [58,59] can reduce CO_2 emissions when looking at the system holistically.

Accordingly, in this section, the authors present Section 2.1, where HTA demands are modelled; Section 2.2, where energy supply models and the related plant arrangement are discussed; Sections 2.3 and 2.4, where overall CO_2 emissions and costs are evaluated; and finally, Section 2.5, where the model for blending H_2 into CH_4 main fuel stream is presented.

2.1. Energy consumption model for Hard-to-Abate sectors

The proposed model aims to provide a robust and, at the same time, easy-to-adapt approach for evaluating energy consumption and requirements of HTA sectors. Indeed, to meet their production capacity (C_P), heat and electricity are required. To give a broader scope of the model, cold energy and water demands have also been included, looking for instance at cement plant batching sections [28,60] and refineries [61] where up to 4% of the overall operating cost is strictly linked to water usage. The model integrates a comprehensive database featuring up-to-date and sector-specific energy consumption metrics for HTA industries to capture these complexities, as discussed in the introduction. The fact that the model relies on the actual numbers related to existing processes is essential for accurately predicting the overall HTA sector consumption. The modelling approach proposed in this section accounts for the breakdown of multiple processes where the overall HTA sector demands are evaluated summing up the demands required by each process. The schematic representation of the model is shown in Fig. 1.

To classify among the different HTA processes which are the ones that can be electrified, cogenerated and decarbonised, the authors proposed, based on the SoA analysis of the most up-to-date generating technologies (namely heat pumps, CHP, boilers, etc.), a systematic breakdown of the heat consumptions into three contributions, in respect of the temperature level [29,62] Accordingly, the heat demand (H^D) is systematically broken down into contributions from processes operating at low (T ∈ [70; 150] °C), medium (T ∈ [150; 400] °C), and high (T ∈ [400; T_{MAX}] °C) temperature ranges, labelled as Low Temperature (LT), Medium Temperature (MT), and High Temperature, respectively.

The total heat demand is computed as the sum of individual contributions from all HT, MT, and LT processes, as per Eq. 2. Similarly, the model evaluates electricity (E^D), cold energy (C^D), and water (W^D) demands, factoring in the specific number (N_j) of processes that require these resources. According to the data found in other studies [63], cold energy demand considers processes that operate within a defined temperature range (T ∈ [0; 20] °C), while water demand is tied to the process's dependent on water usage.

This comprehensive approach provides a granular understanding of energy consumption within HTA sectors and helps identify opportunities to optimise overall energy efficiency and reduce carbon emissions. Starting from the sector production C_P, and thanks to specific consumptions ($H_{SC}, E_{SC}, C_{SC}, W_{SC}$) provided by the database in [kWh/Ton_P] and [m^3/Ton_P], it is possible to evaluate for each demand and of each process *j-th*, the related demands as per the functional equation given in Eq. 1:

$$f\left(C_P, H_{SC}, H^D, E_{SC}, E^D, C_{SC}, C^D, W_{SC}, W^D\right)\Big|_j = 0 \tag{1}$$

Starting from Eq. 1, the model allows for the evaluation of the overall H_K^D as per:

$$H_K^D = \sum_{j=1}^{N_{HT}} H_{jk}^{D_{HT}} + \sum_{j=1}^{N_{MT}} H_{jk}^{D_{MT}} + \sum_{j=1}^{N_{LT}} H_{jk}^{D_{LT}} \tag{2}$$

where N_{HT}, N_{MT} and N_{LT} represent the number of HT, MT and LT processes of the *k-th* HTA sector. Similarly to H_K^D, the electricity consumption of the *k-th* HTA sector E_K^D is computed according to (3), with respect

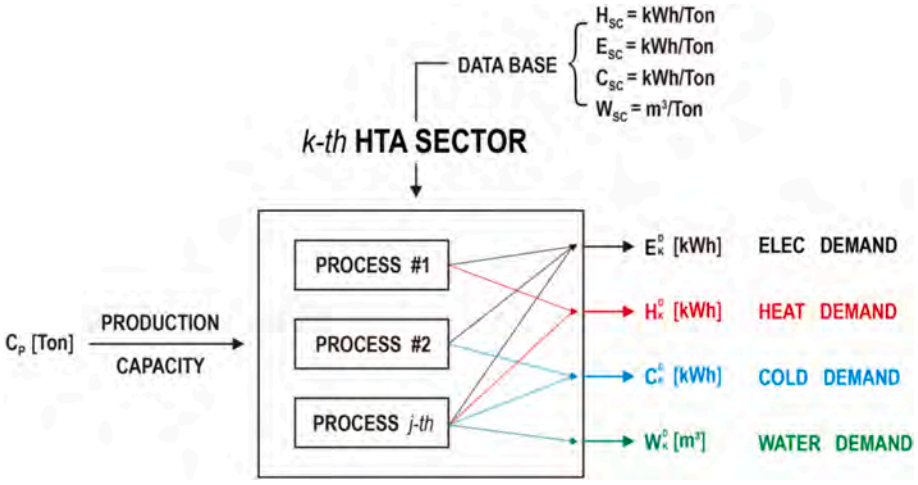

Fig. 1. *k-th* Hard-to-Abate sector – energy consumption model.

to the number of processes N_E requiring electricity:

$$E_K^D = \sum_{j=1}^{N_E} E_{jk}^D \tag{3}$$

Cold energy and Water demands, included for giving generality to the model, are evaluated according to Eqs. (4) and (5):

$$C_K^D = \sum_{j=1}^{N_C} C_{jk}^D \tag{4}$$

$$W_K^D = \sum_{j=1}^{N_W} W_{jk}^D \tag{5}$$

where N_C and N_W are the number of processes of the *k-th* HTA sector requiring cold energy and water, respectively.

Following this approach, it is possible to integrate different processes and subsequent HTA sectors, evaluating the overall demands of electricity, heat, cold energy, and water to be supplied to the overall industrial district.

2.2. Energy supply model for the Hard-to-Abate sectors

Looking at the holistic integration of smart multi-energy systems [2] into industrial districts, the authors proposed a methodological approach based on an energy supply model that integrates multiple technologies to generate electricity, heat, cold energy and water. The scheme of the proposed model is shown in Fig. 2, where among the available technologies, the authors selected the most adopted such as combined heat and power (CHP) systems, Power Plants (PP), RES plants, boilers (BO), heat pumps (HP), vapour compression chillers (VCCH), absorption chillers (ABCH), and reverse osmosis (RO) systems.

The proposed modular approach based on 0-D grey-box, steady state component model simulation, allows for scalability across different HTA sectors, from small-scale facilities to large industrial complexes, and approaching the conceptualisation of smart industrial districts where different end-user demands could be satisfied from centralised energy systems and eventually by sharing electricity, heat, cold energy and water among district concept. The energy supply model emphasises the

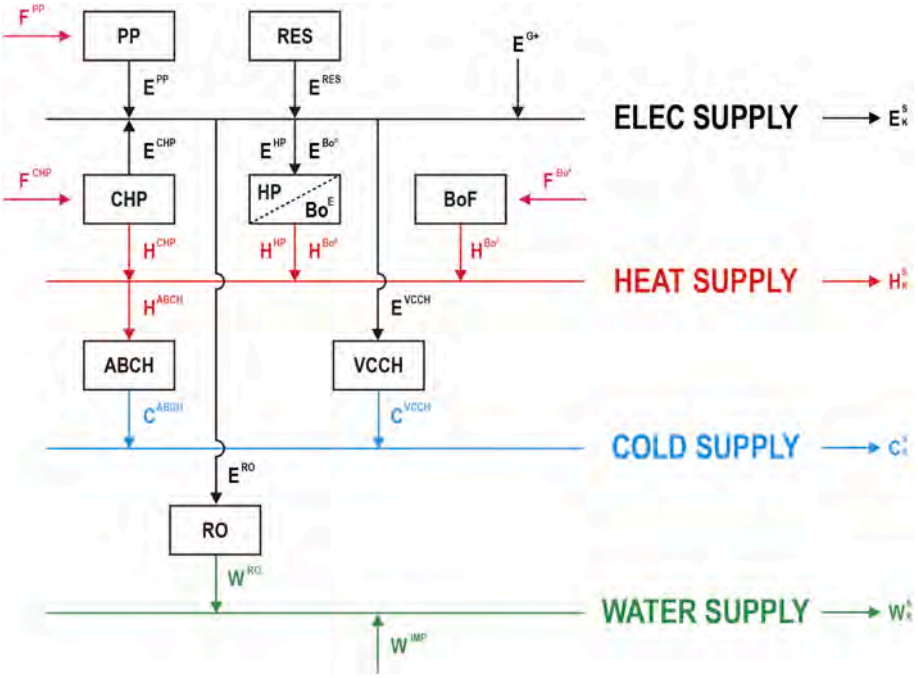

Fig. 2. Energy supply model for Hard-to-Abate sector demands.

integration of diverse energy generation technologies to meet the demands of HTA sectors both from an efficient point of view and from a ready-to-developed approach, where existing technologies can be integrated and eventually retrofitted in the various plant configurations. Indeed, to optimally tailor the solution to real plant solutions, the different models include performance metrics such as efficiencies and coefficient of performance (e.g., η_J, COP_J) to reflect technology-specific characteristics accurately.

Each model, and consequently the overall energy supply model, is formulated through a series of equations representing the conservation of mass and energy, and each component behaviour through key performance metrics, such as efficiencies and coefficients of performance. Accordingly, and with reference to the nomenclature and schematic representation given in Fig. 2, the equation representing the energy supply model are proposed.

The model accounts for the conservation equation definition for each bus (network), where energy conservation is guaranteed for electricity, heat, and cold energy supply, while mass conservation is for the water supply.

Electricity supply for the *k-th* HTA sector bus is fully described by Eq. 6:

$$E^S{}_k = \sum_{j=1}^{N_{G+}} E_j^{G+} + \sum_{j=1}^{N_{CHP}} E_j^{CHP} + \sum_{j=1}^{N_{PP}} E_j^{PP} + \sum_{j=1}^{N_{RES}} E_j^{RES} - \sum_{j=1}^{N_{HP}} E_j^{HP} - \sum_{j=1}^{N_{BOE}} E_j^{BOE} - \sum_{j=1}^{N_{VCCH}} E_j^{VCCH} - \sum_{j=1}^{N_{G-}} E_j^{G-} - \sum_{j=1}^{N_{RO}} E_j^{RO} \quad (6)$$

where E_j^{CHP}, E_j^{PP} *and* E_j^{RES} represent the electricity generated by the *j-th* CHP, *j-th* PP and *j-th* RES plant, respectively, and E_j^{G+} the electricity imported from the grid. E_j^{BOE}, E_j^{HP}, E_j^{VCCH} and E_j^{RO} are the electricity demands to operate the BO_E, HP, VCCH and RO component. The model accounts also for the electricity that can be exported E_j^{G-}.

The heat supply bus is described by Eq. 7.

$$H^S{}_k = \sum_{j=1}^{N_{H+}} H_j^{+} + \sum_{j=1}^{N_{BOF}} H_j^{BOF} + \sum_{j=1}^{N_{HP}} H_j^{HP} + \sum_{j=1}^{N_{BOE}} H_j^{BOE} + \sum_{j=1}^{N_{CHP}} H_j^{CHP} - \sum_{j=1}^{N_{H-}} H_j^{-} - \sum_{j=1}^{N_{AC}} H_j^{AC} \quad (7)$$

where the positive terms are related to heat H_j^{CHP} H_j^{HP}, $H_j^{BOF}$and H_j^{BOE}made available by the CHP units, HP, BO_E, and BO_F, respectively. $H_j^{+}$and H_j^{-} are introduced for the generality of the modelling and account for the option that the system imports and exports some heat in the case of district heating layouts.

The cold energy supply bus mainly accounts for the cold energy C_j^{VCCH} and C_j^{ABCH}generated by *j-th* VCCH and ABCH, respectively, and for imported and exported cold energy C_j^{+} and C_j^{-}, if district cooling operations occur in the industrial estate [56]. Eq. 8 expresses the energy conservation on the cold energy bus:

$$C^S{}_k = \sum_{j=1}^{N_{C+}} C_j^{+} + \sum_{j=1}^{N_{VCCH}} C_j^{VCCH} + \sum_{j=1}^{N_{ABCH}} C_j^{ABCH} - \sum_{j=1}^{N_{C-}} C_j^{-} \quad (8)$$

The authors have included the water bus in the model, since in many HTA sectors, water is actively involved in the accomplishment of the production value chain and brings along CO_2 emissions and costs. Accordingly, Eq. 9 shows the mass conservation on the water bus:

$$W^S{}_k = \sum_{j=1}^{N_{RO}} W_j^{RO} + \sum_{j=1}^{N_{W+}} W_j^{+} - \sum_{j=1}^{N_{W-}} W_j^{-} \quad (9)$$

where W_j^{RO} represent the water produced by the RO, and W_j^{+} and W_j^{-} the water imported and exported from the plant.

In addition of the equation set presented from Eqs. 6 to 9, the equations describing the components behaviour in respect of the their performance such as efficiencies, specific consumptions and coefficient of performances have also been presented.

Starting from this approach, the primary fuel consumption accounting for CHP and PP is evaluated in Eq. 10, accounting for the CHP ratio H/E [64,65] that represent how much heat is generated in respected of the electricity. By all means, when dealing with pure PP, H/E is zero. Accordingly, adopting a general formulation given in Eq. 10,

$$F_j^{k_J} = E_j^{k_J} \bullet \left(1 + H_j^{k_J} \Big/ E_j^{k_J}\right) \bullet \frac{1}{\eta_J{}^{k_J}} \quad (10)$$

It is possible to account for both CHP and PP, when $k_J = 1 \& k_J = 2$, respectively, and their related efficiencies. Still, looking at fuel-fed equipment, the fuel boiler equation is summarized in Eq. 11, where the heat generated is related to the boiler primary fuel input $F_J^{BO_F}$ and its efficiency $\eta_J^{BO_F}$:

$$H_J^{BO_F} = \eta_J^{BO_F} \cdot F_J^{BO_F} \quad (11)$$

In the case of the Electric Boiler/Heater and Heat Pumps, the heat generated $H_J^{BO_E}$ and H_J^{HP} are related to the electricity input, $E_J^{BO_E}$ and E_J^{HP}, and to the BO efficiency $\eta_J^{BO_E}$ and to the HP coefficient of performance COP_J^{HP}, respectively:

$$H_J^{BO_E} = \eta_J^{BO_E} \cdot E_J^{BO_E} \quad (12)$$

$$H_J^{HP} = COP_J^{HP} \cdot E_J^{HP} \quad (13)$$

VCCH and ABCH equations are both functions of the coefficient of performance of the related component, while the first is fed with electricity, and the second with heat. Eqs. 14 and 15, show the VCCH and ABCH behaviour, respectively.

$$C_J^{VCCH} = COP_J^{VCCH} \cdot E_J^{VCCH} \quad (14)$$

$$C_J^{ABCH} = COP_J^{ABCH} \cdot H_J^{ABCH} \quad (15)$$

The RO model allows for the evaluation of the amount of water mass W_J^{RO} produced starting from the required electricity E_J^{RO}. The key performance parameter is the specific consumption expressed in m3/kWh. The Eq. 16 represents the RO.

$$W_J^{RO} = C_{S_J}^{RO} \cdot E_J^{RO} \quad (16)$$

According to the overall set of equations that allow for evaluating all the terms and variables presented in Fig. 2, they are later used for evaluating the environmental techno-economic parameters required to perform the simulations.

2.3. Carbon emissions evaluation

To comprehensively evaluate the environmental impact of the energy supply system, the model takes the carbon emissions associated with each flow entering the system into account, ranging from the electricity imported from the grid, the amount of fuel required for feeding the CHP, PP systems and boilers, and accounts also for heat and cold energy imports, looking at industrial district scenarios. Carbon emissions are calculated as the product of energy consumption and the corresponding emission factors. The emission factors, expressed in kilograms of CO_2 per kilowatt-hour ($kgCO_2/kWh$), capture the specific carbon intensity of each primary input. The resulting total emissions are expressed in tons of CO_2 per year. The carbon emission evaluation framework provides a detailed assessment of the environmental impact associated with the energy supply system. Indeed, each emission factor $f_{CO_2}$is specific to each energy input and varies depending on the fuel mix (namely H2-CH4 blending, in the proposed case scenario) and energy generation technologies. The proposed approach is generic in the formulation and, for this reason, can be adjusted appropriately to different HTA sectors, enabling a tailored evaluation of carbon emissions based on sector-specific energy profiles. The proposed granular

approach for accounting for CO_2 emissions allows the model to be easy to link with the most advanced certification standards, ISO 14064/14067 for instance, allowing the entire value chain of the sustainable linked loans and green financing mechanisms [66,67].

CO_2 emissions from total Fuel $CO_2^{F_{TOT}}$ are evaluated from fuel consumption in CHP, PP and BO^F systems and are calculated as Eq. 17:

$$CO_2^{F_{TOT}} = \sum_{j=1}^{N_F^{CHP}} F_j^{CHP} \cdot f_{CO_2}^{CHP} + \sum_{j=1}^{N_F^{PP}} F_j^{PP} \cdot f_{CO_2}^{PP} + \sum_{j=1}^{N_F^{BOF}} F_j^{BOF} \cdot f_{CO_2}^{BOF} \quad (17)$$

CO_2 emissions due to electricity CO_2^E imported from the grid are calculated as Eq. 18

$$CO_2^E = \sum_{j=1}^{N_G^+} E_j^{G+} \cdot f_{CO_2}^E \quad (18)$$

CO_2 emissions due to district heating $CO_2^H$and cooling CO_2^Cconsumption are evaluated as Eqs. 19 and 20

$$CO_2^H = \sum_{j=1}^{N_H^+} H_j^{H+} \cdot f_{CO_2}^H \quad (19)$$

$$CO_2^C = \sum_{j=1}^{N_C^+} C_j^{C+} \cdot f_{CO_2}^C \quad (20)$$

CO_2 emissions due to Water Supply CO_2^W*are* evaluated as Eq. 21

$$CO_2^W = \sum_{j=1}^{N_W^+} W_j^+ \cdot f_{CO_2}^W \quad (21)$$

Accordingly, Total Carbon Emissions CO_2^{TOT} from the system are calculated by summing the individual contributions, as per Eq. 22:

$$CO_2^{TOT} = CO_2^E + CO_2^H + CO_2^C + CO_2^W + CO_2^{F_{TOT}} \quad (22)$$

It should also be highlighted, that despite it has not been taken into consideration in the proposed model, Eqs. 18–21 could also be generalized including for the negative CO_2 emissions thus accounting the options of exporting the generated goods to other players potentially part of the industrial district.

2.4. Economic evaluation: OPEX and CAPEX

The economic performance of the energy system is evaluated through two key financial metrics: Operating Expenditures (OPEX) and Capital Expenditures (CAPEX). OPEX represents the costs associated with the system's operation, including fuel consumption, electricity imports, heat, cooling, water usage, and carbon taxes.

Conversely, CAPEX reflects the initial investment costs required to establish the HTA supply systems, including components and equipment such as CHP units), boilers (Electrical and fuel), heat pumps, vapour compression chillers, absorption chillers, and reverse osmosis.

The OPEX and CAPEX evaluations offer valuable insights into the system's economic performance that will allow future studies to evaluate the environmental techno-economic feasibility of the roadmap towards NZE HTA sectors. Indeed, these metrics provide a quantitative basis for evaluating the trade-offs between initial investment and ongoing operational costs, allowing the formulation of advanced objective functions for ping the HTA supply system design. The authors have proposed an approach based on a proprietary database of equipment costs for evaluating the CAPEX for each system as the product of the specific cost of the technology by the nominal capacity of the related asset, as shown by Eqs. 30 to 36, it is worthy of note that specific CAPEX C_o^{k-th} of the *k-th* components, typically expressed as [*euro/kW*], is representative of the family/class of equipment taken into consideration and can be easily adjusted to be the most adequate value when detailed OEM data are available. On the operational side, the authors have accounted – in this paper – for variable OPEX, related to the consumables such as fuel mass, electricity imported from the grid, and water required by the processes. Following this approach, the formulation of both OPEX and CAPEX equations is adaptable to systems of different scales and configurations, making the methodology versatile for various applications in HTA sectors.

2.4.1. OPEX evaluation

The $OPEX^E$ associate to the electricity imported from the grid E_j^{G+} is calculated as equation Eq. 23, where $\epsilon^E$is the price of the purchased electricity, in the specific case study assumed to be constant over the year.

$$OPEX^E = \sum_{j=1}^{N_G^+} E_j^{G+} \cdot \epsilon^E \quad (23)$$

Similarly, the $OPEX^F$are related to the fuel consumption in CHP, PP and BO^F systems is given by Eq. 24, where ϵ^{CHP}, ϵ^{PP} ϵ^{BOF} represents the fuel cost for CHP, PP and BO_F, which, on a general basis, could differ.

$$OPEX^F = \sum_{j=1}^{N_F^{CHP}} F_j^{CHP} \cdot \epsilon^{CHP} + \sum_{j=1}^{N_F^{PP}} F_j^{PP} \cdot \epsilon^{PP} + \sum_{j=1}^{N_F^{BOF}} F_j^{BOF} \cdot \epsilon^{BOF} \quad (24)$$

$OPEX^H$ and $OPEX^C$, related to the heat and cold energy imported, are established based on the heat and cold energy cost, and the formulation is expressed by Eqs. 25 and 26.

The operational cost of heat imported or consumed is calculated as:

$$OPEX^H = \sum_{j=1}^{N_H^+} H_j^{H+} \cdot \epsilon^{H+} \quad (25)$$

$$OPEX^C = \sum_{j=1}^{N_C^+} C_j^{C+}(t) \cdot \epsilon^{C+} \quad (26)$$

$OPEX^W$ is calculated based on the water imported and of the related unitary cost ϵ^{W+}, and Eq. 27 expresses it.

$$OPEX^W = \sum_{j=1}^{N_W^+} W_j^{W+} \cdot \epsilon^{W+} \quad (27)$$

It is important to highlight the importance of evaluating the OPEX for Carbon Tax $OPEX^{CO2}$. Indeed, the cost of carbon emissions is based on the carbon tax applied to the total emissions, and the carbon tax $\epsilon_{TAX}^{CO_2}$ is a relevant parameter used for the case study investigation.

$$OPEX^{CO2} = CO_2^{TOT} \cdot \epsilon_{TAX}^{CO_2} \quad (28)$$

The total operational expenditures are calculated as the sum of all OPEX components:

$$OPEX^{TOT} = OPEX^E + OPEX^F + OPEX^H + OPEX^C + OPEX^W + OPEX^{CO2} \quad (29)$$

2.4.2. CAPEX evaluation

CAPEX for CHP and PP systems:

The capital cost of CHP and PP systems is proportional to their nominal electrical capacity P_{NOM}^{CHP}, P_{NOM}^{PP}, respectively

$$CAPEX^{CHP} = C_o^{CHP} \cdot P_{NOM}^{CHP} \quad (30)$$

$$CAPEX^{PP} = C_o^{PP} \cdot P_{NOM}^{PP} \quad (31)$$

CAPEX for heat pumps $CAPEX^{HP}$:

The capital cost of heat pumps is proportional to their nominal electrical capacity P_{NOM}^{HP}

$$CAPEX^{HP} = C_o^{HP} \cdot P_{NOM}^{HP} \quad (32)$$

CAPEX for Fuel and Electric Boilers $CAPEX^{BO_F}$ and $CAPEX^{BO_E}$ are evaluated based on the nominal heat power output, $Q_{NOM}^{BO_F}$and $Q_{NOM}^{BO_E}$, respectively.

$$CAPEX^{BO_F} = C_o^{BO_F} \cdot Q_{NOM}^{BO_F} \quad (33)$$

$$CAPEX^{BO_E} = C_o^{BO_E} \cdot Q_{NOM}^{BO_E} \quad (34)$$

CAPEX for Vapor Compression Chillers $CAPEX^{VCCH}$:

The capital cost of vapour compression chillers depends on their

nominal cooling power capacity CP_{NOM}^{VCCH}

$$CAPEX^{VCCH} = C_o^{VCCH} \cdot CP_{NOM}^{VCCH} \quad (35)$$

CAPEX for Absorption Chillers $CAPEX^{ABCH}$:

The capital cost of absorption chillers is calculated based on their nominal cooling power capacity CP_{NOM}^{ABCH}

$$CAPEX^{ABCH} = C_o^{ABCH} \cdot CP_{NOM}^{ABCH} \quad (36)$$

CAPEX for Reverse Osmosis Systems $CAPEX^{RO}$:

The capital cost of reverse osmosis systems is proportional to their nominal water treatment capacity WC_{NOM}^{RO}:

$$CAPEX^{RO} = C_o^{RO} \cdot WC_{NOM}^{RO} \quad (37)$$

CAPEX for RES $CAPEX^{RES}$:

The capital cost of general RES is assumed to be proportional to the RES installed capacity P_{NOM}^{RES}:

$$CAPEX^{RES} = C_o^{RES} \cdot P_{NOM}^{RES} \quad (38)$$

The overall CAPEX is computed as the sum of all terms provided from Eqs. 30 to 38.

2.5. Fuel mixing model

To exploit the potential of decarbonising HTA by blending H2 together with CH4, it is crucial to evaluate the blended fuel-specific properties in terms of LHV, equivalent emission factor $fCO2_{BL}$, and equivalent specific cost per kWh or per kg. Accordingly, the authors have proposed a 0-D lumped model for accomplishing the evaluation of the quantities mentioned above. The scheme of the mixer component model is presented in Fig. 3:

From the general approach presented by the authors, the mixer, or 'blender,' is capable of dealing with *k-th* gaseous streams (each characterized by specific chemical and physical properties) into a blended flow stream. Given the steady-state condition of the processes and the authors' requirement of system global performance evaluations, the model is simplified, and it assumes that the blending process is isobaric (constant pressure) and isothermal (constant temperature) conditions, assuming the system reaches thermodynamic equilibrium, ideally. For this methodology, only mass and energy conservation equations are explicitly considered.

Starting from the various fuel stream's molar fractions (%vol), the mixer model allows the evaluation of the corresponding mass fractions, thanks to Eq. 39,

$$\%m_k = \frac{\%vol_k \cdot PM_k}{\sum_{k=1}^{n}(\%vol_k \cdot PM_k)} \quad (39)$$

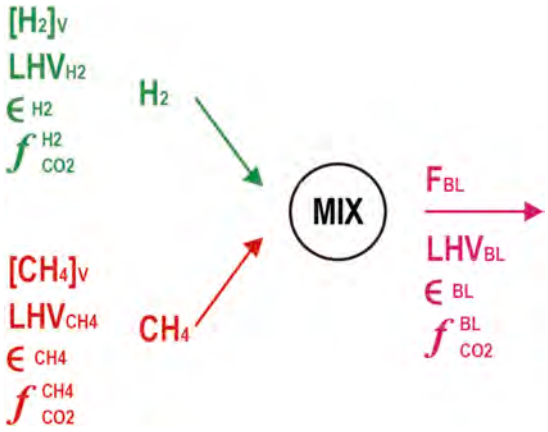

Fig. 3. Fuel mixer component model scheme.

The mass fraction is essential to ensure energy conservation and to quantify thus the blended fuel LHV_{bl}, given in Eq. 40, and the blended fuel emissions factor, $fCO2_{BL}$, shown in Eq. 41, respectively.

$$LHV_{BL} = \sum_{k=1}^{n}(\%m_k \cdot LHV_k) \quad (40)$$

$$f_{CO_2BL} = \sum_{k=1}^{n}\left(\%m_k \cdot \frac{LHV_k \cdot f_{CO_2,k}}{LHV_{BL}}\right) \quad (41)$$

Looking at the system cost, the blended fuel cost is provided by Eq. 42

$$\epsilon_{BL} = \sum_{k=1}^{n} \%m_k \cdot \frac{LHV_k \cdot \epsilon_k}{LHV_{BL}} \quad (42)$$

The computation of the H_2-CH_4 blending mixture properties have been performed using the fluid properties CoolProp (https://coolprop.org/coolprop/wrappers/MATLAB/index.html#matlab), and the well know REFPROP fluid properties from NIST.

3. HTA supply and demand matching

After having proposed the methodological approach followed for dealing with the integration of multi-energy systems in the decarbonization roadmaps towards 2050 carbon neutrality and having discussed on how to structure a flexible and reliable modelling tool for solving, in this section the authors present the general concept of the basis on top of which different case studies, related to different configurations, can be explored and evaluated, with a wide focus on the H2 penetration on the generation side.

Accordingly, in Fig. 4, the authors have proposed the HTA Industrial District concept and coupled it with the heat and electricity-generating components to match the component models related to the Energy Demand and Supply models. The scheme illustrates a system-level integration of energy supply and demand for Hard-to-Abate industrial sectors, focusing on decarbonization pathways. Based on Table 3, where the authors summarised heat (H) and electric (E) consumptions of the various HTA sectors in the proprietary database, the scheme of Fig. 4 does not include water consumption and cold energy consumption, since in many applications still are not considered as properly HTA assets. Adding other buses (networks), as per the scheme of Figs. 1 and 2, would not have changed the approach. Indeed, different *k-th* HTA sectors, such as Oil&Gas, Steel Manufacturing, Glass and Paper production, and many others, can be linked together to a Heat Demand and Electric Demand bus, respectively, where j-th generation assets such as CHPs, PPs, HPs, BO_S^E, BO_S^F and the National Grid are injecting the required supply heat and electricity to satisfy the overall demand of the various HTA sectors. It should be remarked that in some industrial specific applications, internal grids provide for supporting the satisfaction of the related demands.

The diagram emphasizes the potential integration also of renewable energy sources coupled with the above-mentioned components, that are fed by electricity from the national grid (or from internal grid) and by a fuel mix (MIX) including hydrogen (H_2), methane (CH_4), Through energy conversion processes, they synergically contribute in injecting heat and electricity into the respective demand buses. This conceptual framework highlights the critical role of flexible, multi-energy systems in decarbonizing HTA sectors while leveraging clean energy carriers like hydrogen to reduce emissions and enhance sustainability.

In order to perform an optimal selection of the proposed plant components, it is relevant to establish also the technical specification of each technology, and the capability of each sub-system to provide the heat at the required temperature level. For doing so, it is worthy of note that despite a single-line Heat Demand bus, according to Eq. 2, together with the overall amount of heat to be supplied expressed in kWh, information related to the temperature and pressure levels, together with related mass, are required to design the generating assets properly.

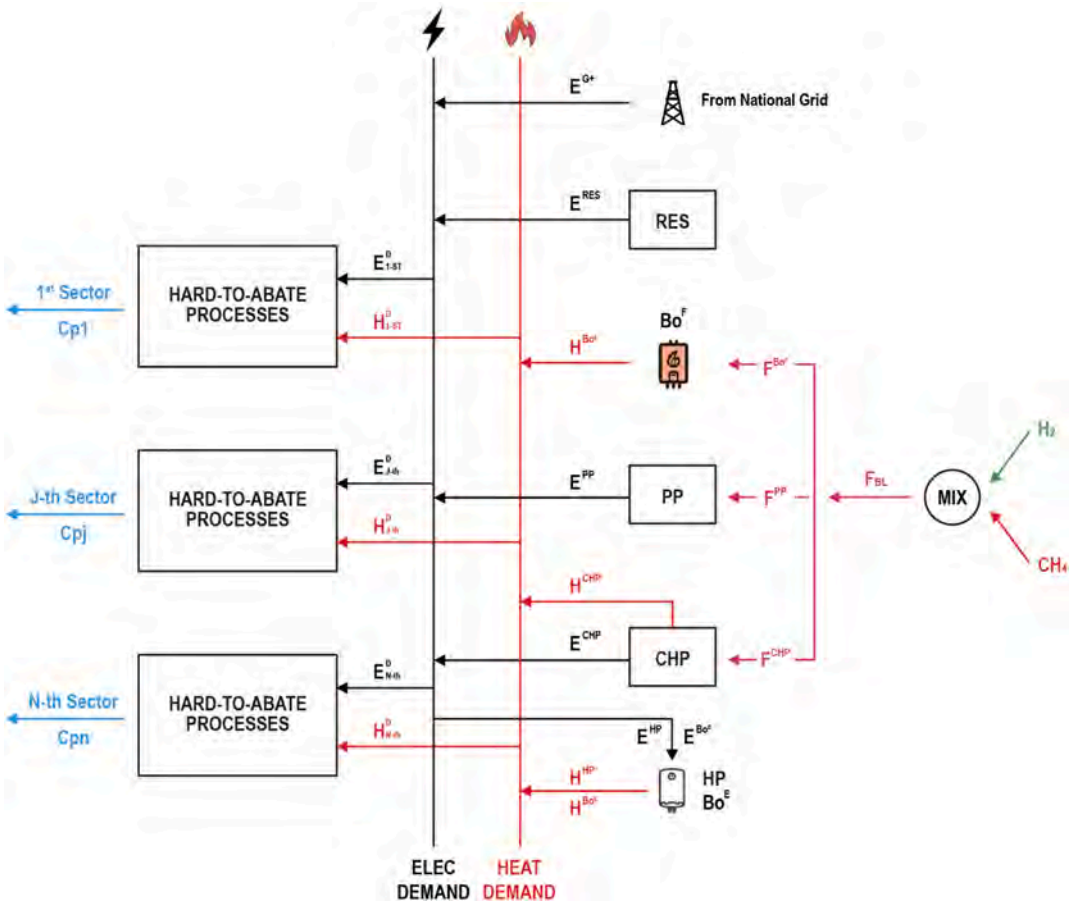

Fig. 4. HTA industrial district concept.

Indeed, heat is generally produced at low, medium and high temperature levels, and for each level, pressure and temperature required to be defined. Indeed, by combining Eqs. 3 and 6, it is possible to define the constraint given in Eq. 43 to guarantee that the HTA sector demands are fully satisfied.

$$\sum E_K^D - \sum E_K^S \leq 0 \tag{43}$$

According to the above, looking at the general configuration of the Heat Demand bus, the Eq. 44 need to be combined with the quality of heat typically generated by the energy system components. Indeed, ranging between HP & BO^E, CHP, and BO^F the heat generated can supply low temperature, medium temperature and high temperature. Thus, as a general modelling approach for breaking down the heat demands in low, medium and high temperature level the authors have defined Eqs. 45–47, where each temperature level is properly combined with technology capable to supply such temperatures and pressures.

$$\sum H_K^D - \sum H_K^S \leq 0 \tag{44}$$

$$\sum H_K^{D_{HT}} - \sum H_K^{BO_F} \leq 0 \tag{45}$$

$$\sum H_K^{D_{MT}} - \left(\sum H_K^{CHP} + \sum H_K^{BO_F}\right) \leq 0 \tag{46}$$

$$\sum H_K^{D_{LT}} - \left(\sum H_K^{BO_E} + \sum H_K^{HP} \sum H_K^{CHP} + \sum H_K^{BO_F}\right) \leq 0 \tag{47}$$

The characterization of temperature levels across various processes and the alignment with corresponding generation technologies are not explored in this paper. The study focuses on evaluating the practical impact of H_2 Levelized Cost of Hydrogen (LCOH) and related emission factors on decarbonizing the overall heat demands of different HTA sectors. This evaluation excludes the integration of Combined Heat and Power (CHP) systems, Heat Pumps (HPs), and Boilers (BOE) in the specific case study. In the following section, the authors present the details of the specific case study, along with a comprehensive list of assumptions and the results of integrating alternative energy carriers, such as H_2, into HTA sectors.

4. Case study

In this paper, the authors have investigated the integration of H_2 energy carriers for H demand-supply, assuming that the CH_4 replacement in heat generation requires only minor technical plant adjustments [68]. This option can be seen as an 'easy-to-implement' alternative that will allow a quick and responsive answer to the request for decarbonising HTA sectors.

To perform the calculation, it has been assumed that electricity demand is fully imported from the national grid, while the heat demand is generated by fuel boilers, fed with H_2-CH_4 blended fuel. Fig. 5, is a specific possible configuration of the general HTA layout presented in Fig. 4, which can be evaluated by considering a reduced sub-set of equations of the one proposed in the Section 2, in the energy demand and supply models.

The evaluations carried out and presented by the authors refer to H_2 production between 1 and 11 (from Table 2), since the other production from 12 to 16 provide similar results since they all refer to CO_2 Neutral Biomass processes. H_2-CH_4 blending between 0% and 100% have been investigated, and results in terms of decarbonization potential operating cost variation have been presented in absolute value per unit of production capacity and also in relative value of CO_2 emissions and operating costs versus the baseline. The benchmark adopted for establishing

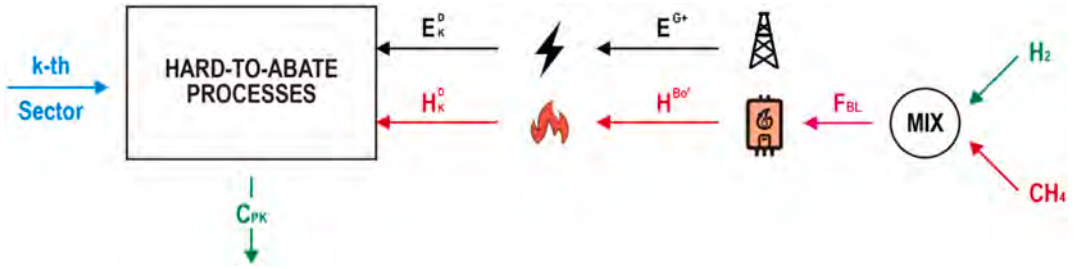

Fig. 5. Fuel mixer component model scheme.

the potential for decarbonising the different proposed configurations refers to specific emissions and costs in Table 3, and results are presented for each of the HTA sectors listed in Table 3. The next section lists the assumptions proposed by the authors based on the most up-to-date SoA for performing the simulations. By all means, by changing the numerical values of the assumptions, the results will change, but the outcome of the proposed model will remain valid.

Assumptions

To perform the evaluation, according to the mathematical formulation proposed in Section 2, and the scheme given in Fig. 5, it is necessary to list assumptions related to electricity and fuel costs, emissions factors, efficiencies and carbon tax. Accordingly, the most relevant assumptions have been listed below:

- The model operates under steady-state conditions without considering transient phenomena.
- Chemical reactions are considered at equilibrium.
- Heat demand (H): the boiler efficiency for H_2 and CH_4 is assumed to be the same [69]
- H_2 Specific emissions (H2 f_{CO2}) and H_2 Specific cost (namely LCOH) refer to values summarized in Table 4, based on the database provided in Table 2. The assumptions of the calculations account for the minimum specific emissions value and to the LCOH values that have been found to be most recurrent in the context. It should be remarked that specific emissions refer to the terms accounted under Scope 1.
- Carbon Tax: 100 €/ton CO_2.
- National Grid: The emission factor assumed of 0.319 kg CO_2 /kWh, according to 2023 Italian data [70,71], price is up to 275.0 €/MWh.
- CH_4: emission factor of 0.210 kg CO_2 /kWh, price is of about 70.0 €/MWh [72]

5. Results & discussion

In this section, the authors present the results of the application of the fuel mixing model, showcasing the blending potential based on the H2 blending ratio through a blended fuel-specific CO_2 emission factor and specific cost maps in Section 5.1. While taking into consideration the plant configuration, together with the technological constraints, such as the boiler efficiency, the blending potential and the benchmark of the various HTA sectors, the effect of the H2 blending in the HTA sectors is fully described in Section 5.2.

Table 4
H2 assumptions for the calculations based on Table 2.

Source	N	Production Method	H2 cost [EUR/MWh]	H2 fCO2 kgCO2/MWh
Methane	1	SMR	57.1	240.2
	2	SMR + CCUS	72.1	60.1
	3	PYROLYSIS	57.1	126.1
Coal	4	GASSIFICATION	42.0	540.5
	5	GASSIFICATIONS + CCUS	141.1	90.1
Electricity (+ water)	6	ELECTROLYSIS BY NUCLEAR	201.2	3.0
	7	ELECTROLYSIS BY ON -SH WIND	342.3	0.0
	8	ELECTROLYSIS BY OFF -SH WIND	318.3	0.0
	9	ELECTROLYSIS BY SOLAR PV	267.3	0.0
	10	ELECTROLYSIS BY GRID	363.4	477.5
Biomass	11	PYROLYSIS	63.1	0.0

5.1. H2 blending potential

To fully exploit the introduction of H2 in the electricity and heat generation of the required HTA demands, it is essential to understand the effects of blending H2 and CH4 on blended fuel LHV, emission factor, cost and decarbonization potential. Indeed, as per the Mixer component model, described in Section 2, it results clear that the evaluation of the above-mentioned quantities strictly depends on the blending ratio, expressed typically in volume ratios, and on the molecular weight of each of the mixture's components (in this case only H2 and CH4). Indeed, as can be observed in Fig. 6, where the x-axis represents the volumetric fraction of H2 in the fuel mixture, the H2 mass fraction becomes greater than the CH4 ones only for volumetric values above 85%. Indeed, the H2 molecular weight is roughly 1/8 of the CH4 molecular weight. Since LHV evaluation and emission factors evaluation are based on the mass composition of the fuel mixture, it can be observed that, considering a CH4 LHV of 13.8 kWh/kg, when a blending in volume of 50% is considered, the blended LHV is of about 16.1 kWh/kg, with an 11% H2 mass fraction in the mixture and an equivalent emission factor, considering the case of Green H2, characterised by 0.0 $kgCO_2$/kgH2, of about 0.16 $kgCO_2$/kWh. By all means, if other H2 production technologies are accounted for, the blended fuel emissions factor will never be 0.0, and Fig. 8 will show this aspect.

From an economic standpoint, thanks to the support of Fig. 7, it can be understood that assuming the CH4 cost of 70 EUR/MWh and the optimistic scenario of the Green Hydrogen at the lowest range of Table 2, with an LCOH of about 4 EUR/kgH2, corresponding to about 118.3 EUR/MWh, also when CO_2 Tax is accounted for, the overall cost of operating the system with H2, is in all the blending scenario, ranging from 10% to 100%, greater than the reference scenario, where volumetric fraction of H2% is 0. It can be observed that the spread on the CO_2 cost, considering a CO_2 tax of 100 EUR/ton, between the reference case scenario and each blending configuration is reducing proportionally with the blending ratio (green candle of the chart), but at that price of the CO_2 tax, is still more expensive than the reference scenario. When the CO_2 tax becomes greater than 200 EUR/ton, the H2 penetration for the given price starts to be convenient.

Given the multitude of parameters affecting the evaluation of the blended fuel emission factors and related costs, the authors have proposed a systematic approach based on maps in Figs. 8, 9 and 10. Indeed, starting from the H2 production database, given in Table 2, the potential combination between H2 specific emission factor, expressed in $kgCO_2$/MWh, and H2 specific costs, expressed in EUR/MWh, it is possible to establish once assumed the CH4 specific emission factor and specific cost, in this case, 210 $kgCO_2$/MWh and 70 EUR/MWh, respectively, which are the values assumed by the blended fuel varying the blending

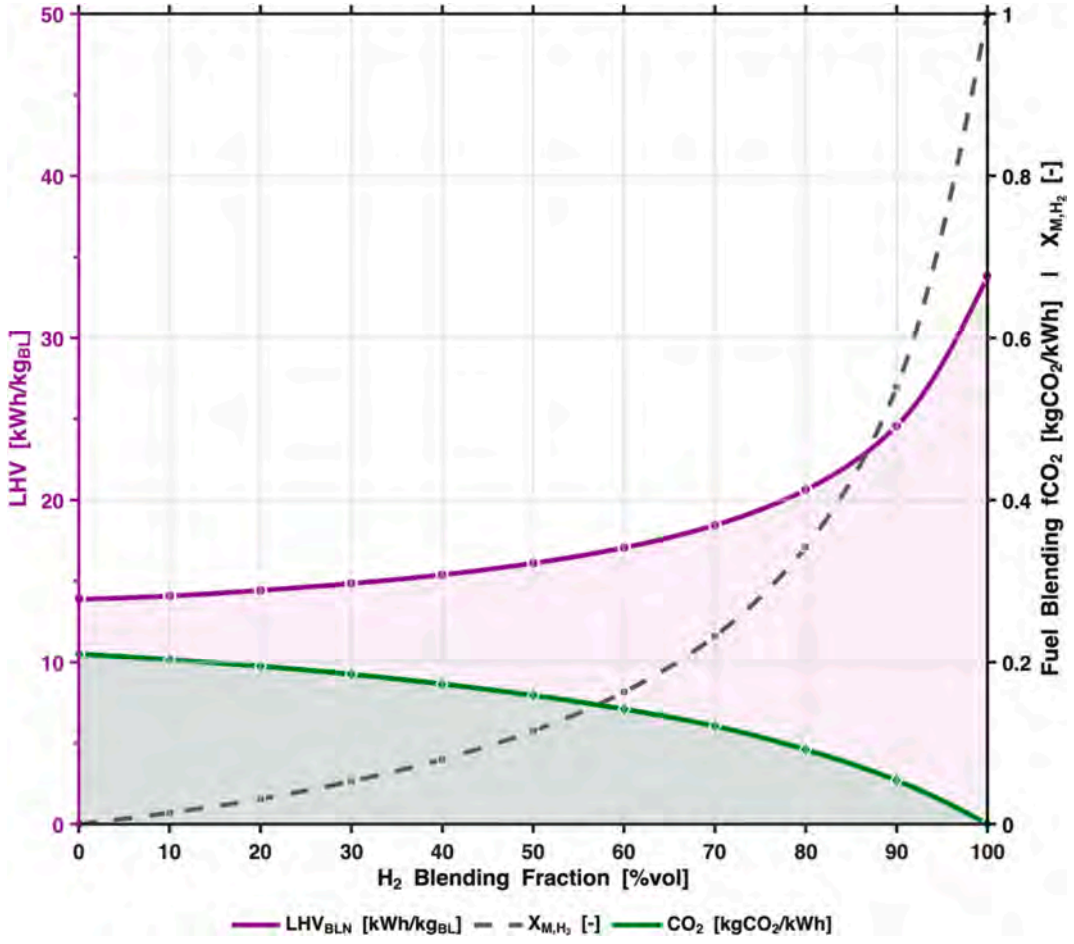

Fig. 6. H2-CH4 blending – LHV, fCO_{2BL} and H2mass vs H2 volumetric fraction.

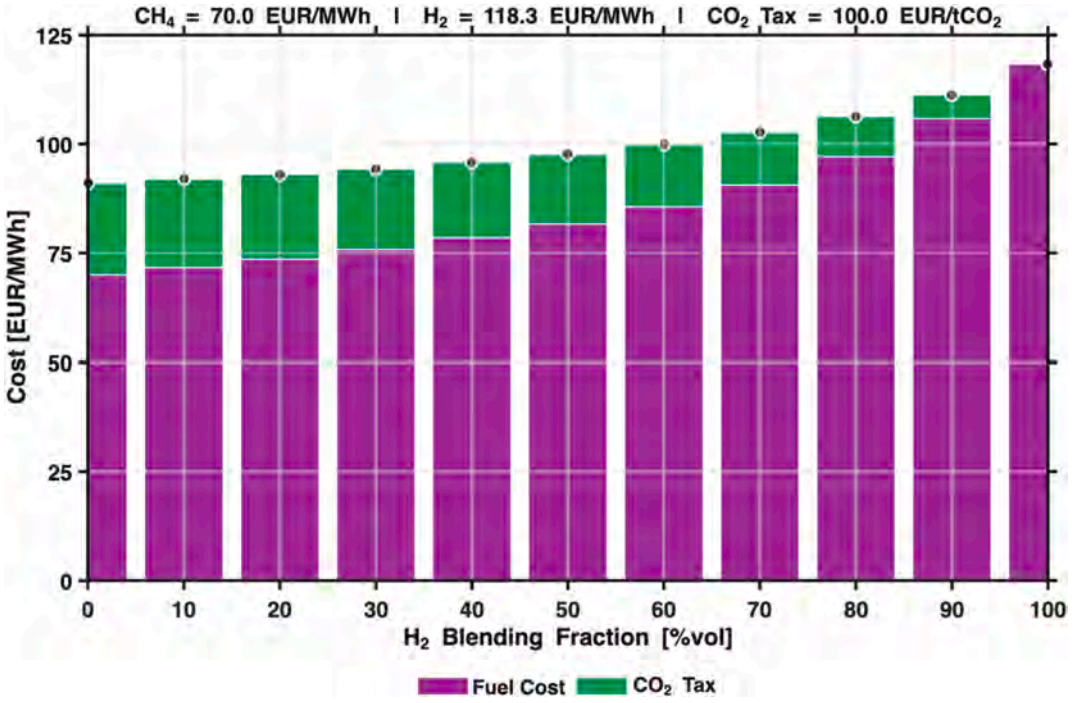

Fig. 7. H2-CH4 blending in volume– blended fuel cost and CO_2 Tax vs H2 volumetric fraction.

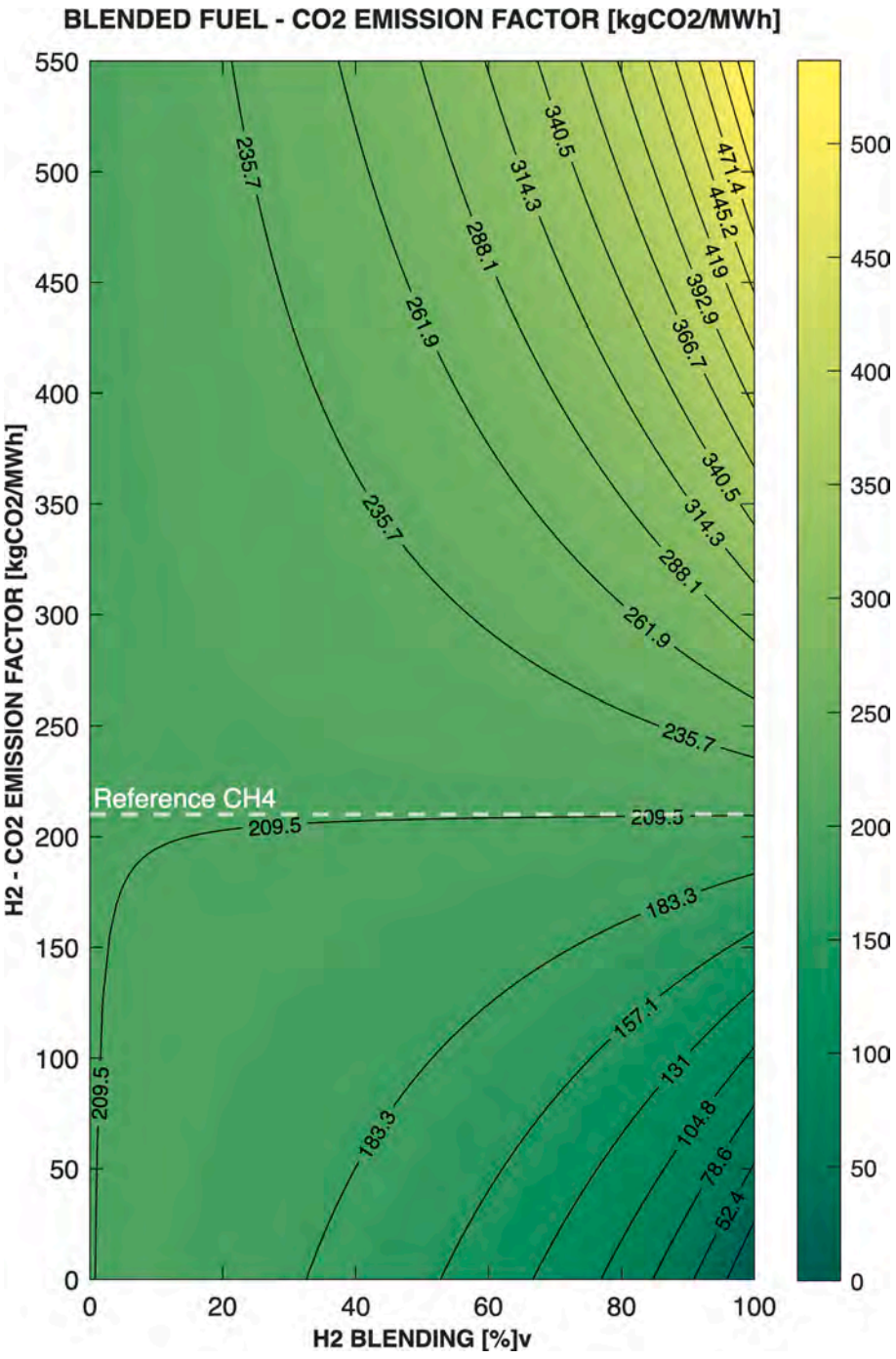

Fig. 8. H2-CH4 blending in volume – blended fuel emission factor map.

ratio, x-axis, and varying the H2 specific emission factor, y-axis of Fig. 8, and the H2 specific cost, y-axis of Figs. 9 and 10, that differ for the assumption of the CO_2 Tax value, that is in one case 0.0 EUR/Ton and in the other case 100.0 EUR/ton. Looking at the CO_2 Emission Factor Map given in Fig. 8, it can be observed that when considering an H2 emission factor equal to zero, varying the blending ratio between 0% to 100%, the blended fuel emission factors are the ones given in Fig. 6.

This map becomes more and more useful when, for instance, a reference emission factor, 210 kgCO2/MWh (ideal combustion of solely CH4), is known, and the decarbonisation target is set. Indeed, if, as an example, a target reduction of 20% is required, leading to about 165–170 kgCO2/MWh, this map helps understand the required blending for a well-established H2 production technology. Furthermore, when coupling H2 integration with energy systems, understanding the technological limitations in accommodating H2 blending becomes fundamental. Looking at Fig. 8, the 20% CO_2 emission factor reduction can be obtained for instance, with a 50% blending of fully Green H2 (emission factor = 0.0), or with a 70% blending of a Blue H2, such as the one given in Table 2, of a Coal Gasification with CCS (emission factor = 90 $kgCO_2$/MWh). Since both options allow for obtaining the same blended fuel emission factor, it becomes relevant to understand, from the economic point of view, how the two different fuels have a practical impact on the system operating costs.

When considering the Green H2, on the basis of the data provided in Table 2.0, in the best-case scenario, the lowest cost is about 120 EUR/MWh of H2, and the highest value is up to 360 EUR/MWh. The Blue H2,

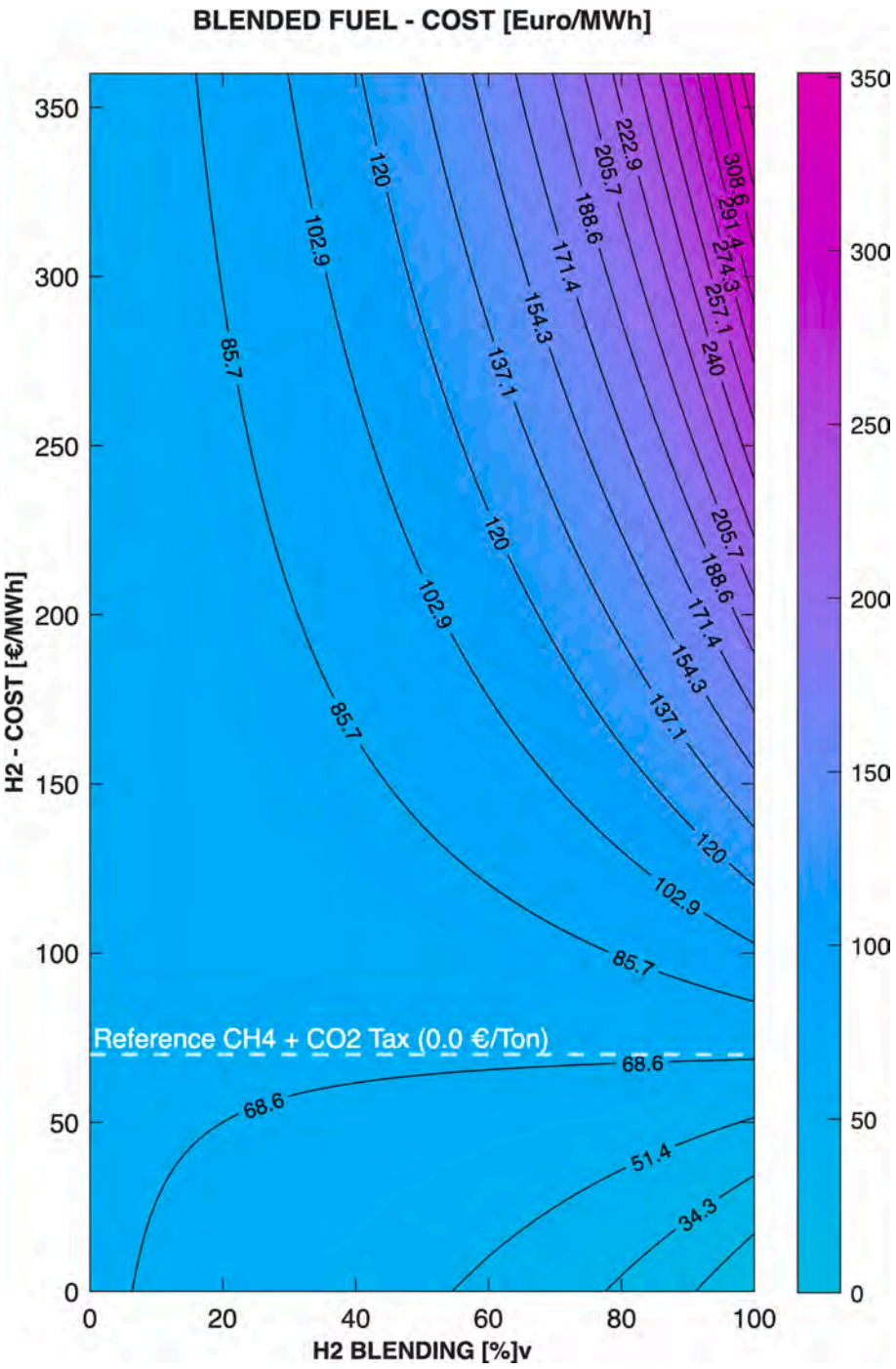

Fig. 9. H2-CH4 blending in volume – blended fuel cost map CH4 Cost = 70 €/MWh & CO_2 Tax = 0.0 EUR/Ton.

instead, ranges between 60 EUR/MWh, in the best scenario, up to 150 EUR/MWh, in the worst, the most expensive. Inputting the H2 Blending Value described before in the Cost map given in Fig. 9, for accomplishing a 20% CO_2 Emission Factor reduction, it can be observed that with the 50% blending ratio (enough when considering Green H2), the blended cost ranges between 80 and 140 EUR/MWh, in respect of the lowest/highest cost given in Table 2, higher than the reference 68 EUR/MWh of the CH4. When considering the Blue H2 and entering the Cost Map with 70% blending, the blended fuel cost ranges between 68 and 102 EUR/MWh, becoming slightly competitive in the best scenario, with the reference case.

Thanks to the support of the Cost Map given in Fig. 10, which includes a CO_2 tax of 100 EUR/Ton CO_2, the blended fuel cost for Green H2 and Blue H2 ranges respectively between 90 and 145 EUR/MWh, and 80 and 115 EUR/MWh, when the reference case scenario is now characterised by an overall reference cost of about 90 EUR/MWh, based on 70 EUR/MWh for the CH4 cost, and about 21 EUR/MWh for accounting the CO_2 Tax.

As seen in this second scenario, when CO_2 Tax is included in the investigation, H2 penetration becomes a valid potential alternative to decarbonise, allowing a comparable economic viability of the solution.

5.2. *Heat supply via H2 in the HTA sectors*

In this section, the authors present the results of the proposed methodology to evaluate the impact of H_2 penetration in the various

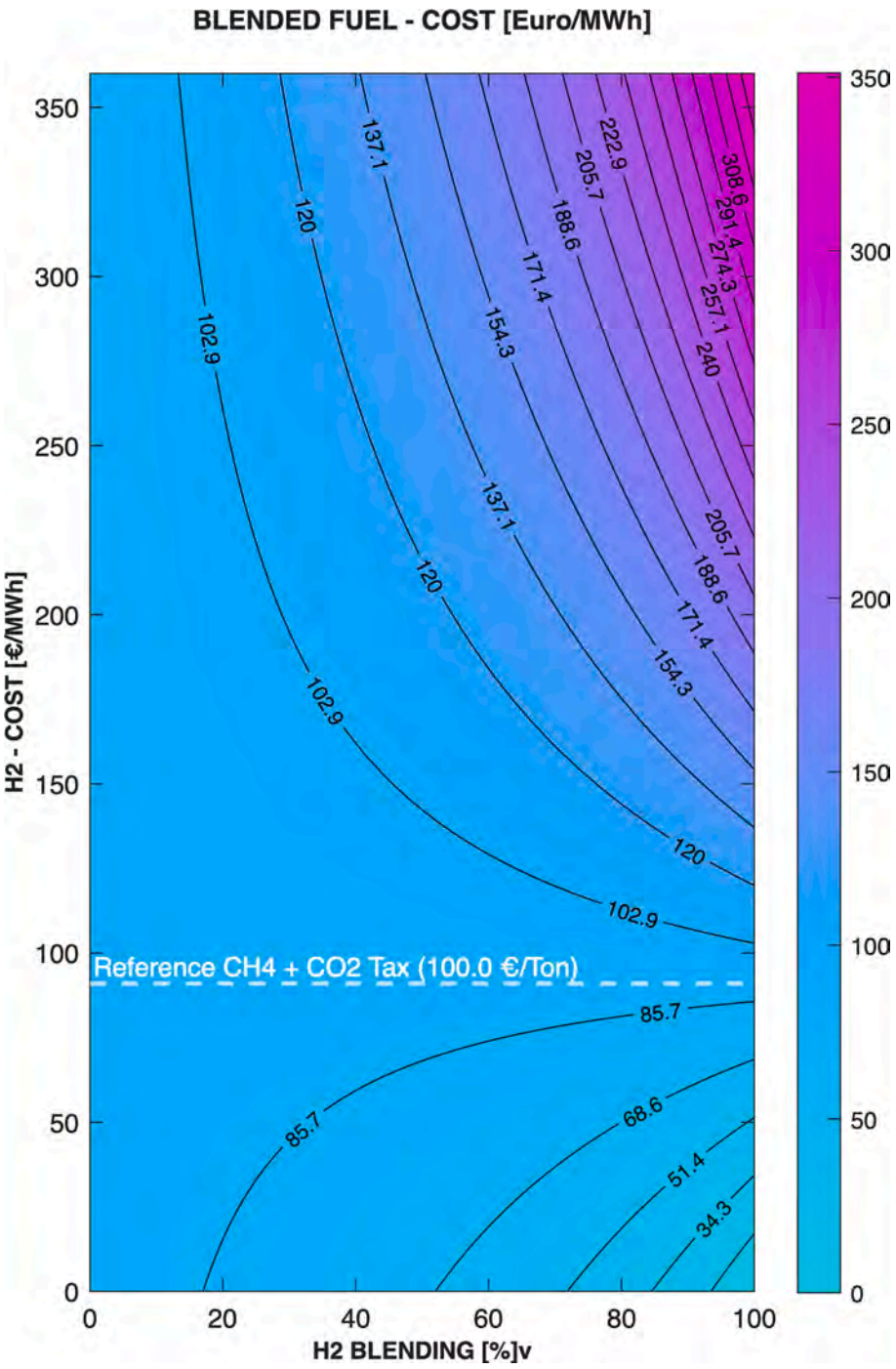

Fig. 10. H2-CH4 blending in volume – blended fuel cost map CH4 Cost = 70 €/MWh & CO_2 Tax = 100.0 EUR/Ton.

HTA sectors, explicitly accounting for the type of H_2 (green, blue, grey, etc.) adopted to tackle the decarbonization challenge. As mentioned before, the reference emission values and costs for generating heat and electricity in each HTA sector are summarized in Table 4 and are used as reference to establish the benchmark conditions. To properly read the proposed CO_2 maps, it is first necessary to recall the reference emission level associated with conventional heat production. Assuming a boiler efficiency of 0.9 and a CH_4 emission factor of 210 $kgCO_2$/MWh, the specific emissions, under Scope 1, for 1 MWh of generated heat are approximately 230 $kgCO_2$. Consequently, if the specific CO_2 emissions associated with a given H_2 production technology led to an effective emission factor for heat production larger than this value, that technology should be not consider a viable alternative, since its use would increase the overall emissions compared to the baseline CH_4-only configuration.

Anyhow, given the importance of mapping the decarbonization potential related to H_2 integration into HTA sectors, the authors, following up with proposed methodology summarized by Fig. 8, 9 and 10, have mapped all the combination of H_2 blending in respect of production costs and associated emission factors, in Fig. 11 and Fig. 12. To account for the threshold benchmark, related to the CO_2 emission reduction viability, of 230 $kgCO_2$/MWh of heat generated, the authors have presented the results in Fig. 13.

Fig. 11 shows the absolute values of total CO_2 emissions $kgCO_2$/ton and total operating costs €/ton as a function of H_2 blending and H_2 quality, while Fig. 12 shows the normalised variation of total operating

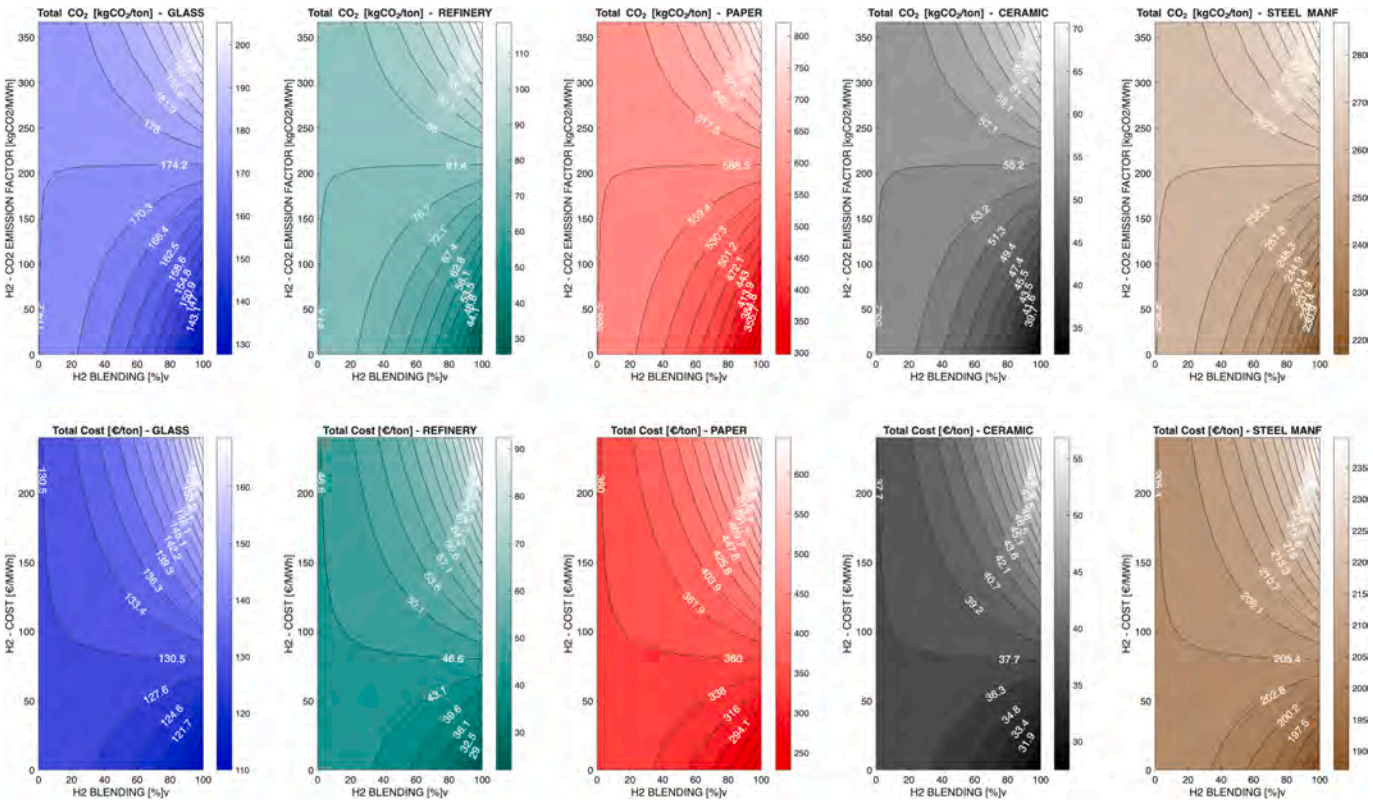

Fig. 11. H2 blending impact on HTA sectors – CO2 emissions and OPEX (absolute values).

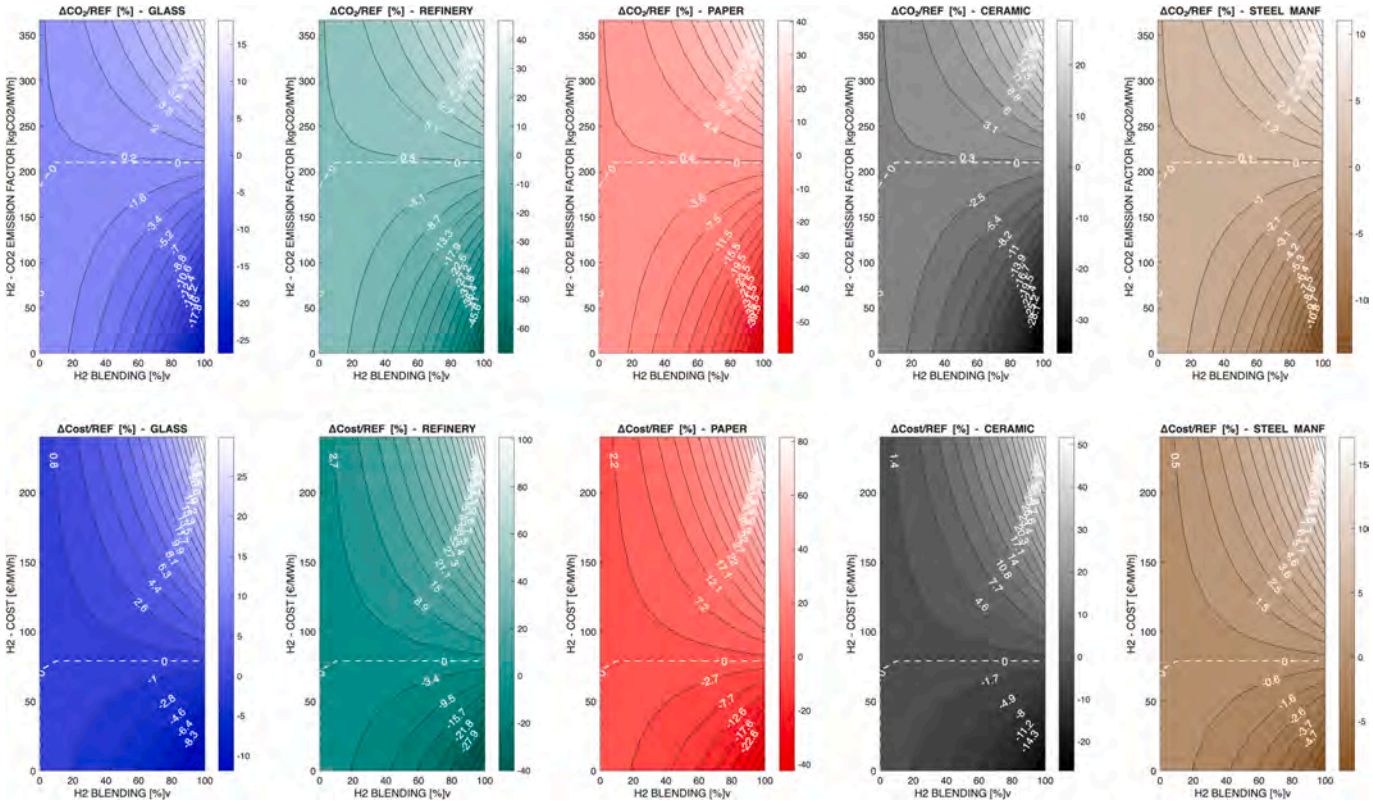

Fig. 12. H2 blending impact on HTA sectors – CO2 emissions and OPEX (normalized values).

cost (ΔCost/REF) and total CO_2 emissions (ΔCO_2/REF) for the five HTA sectors as a function of two independent variables: the volumetric H_2 blending ratio in the fuel mixture (x-axis) and either the specific cost of H_2 €/MWh or its specific emission factor $kgCO_2$/MWh (y-axis). Negative

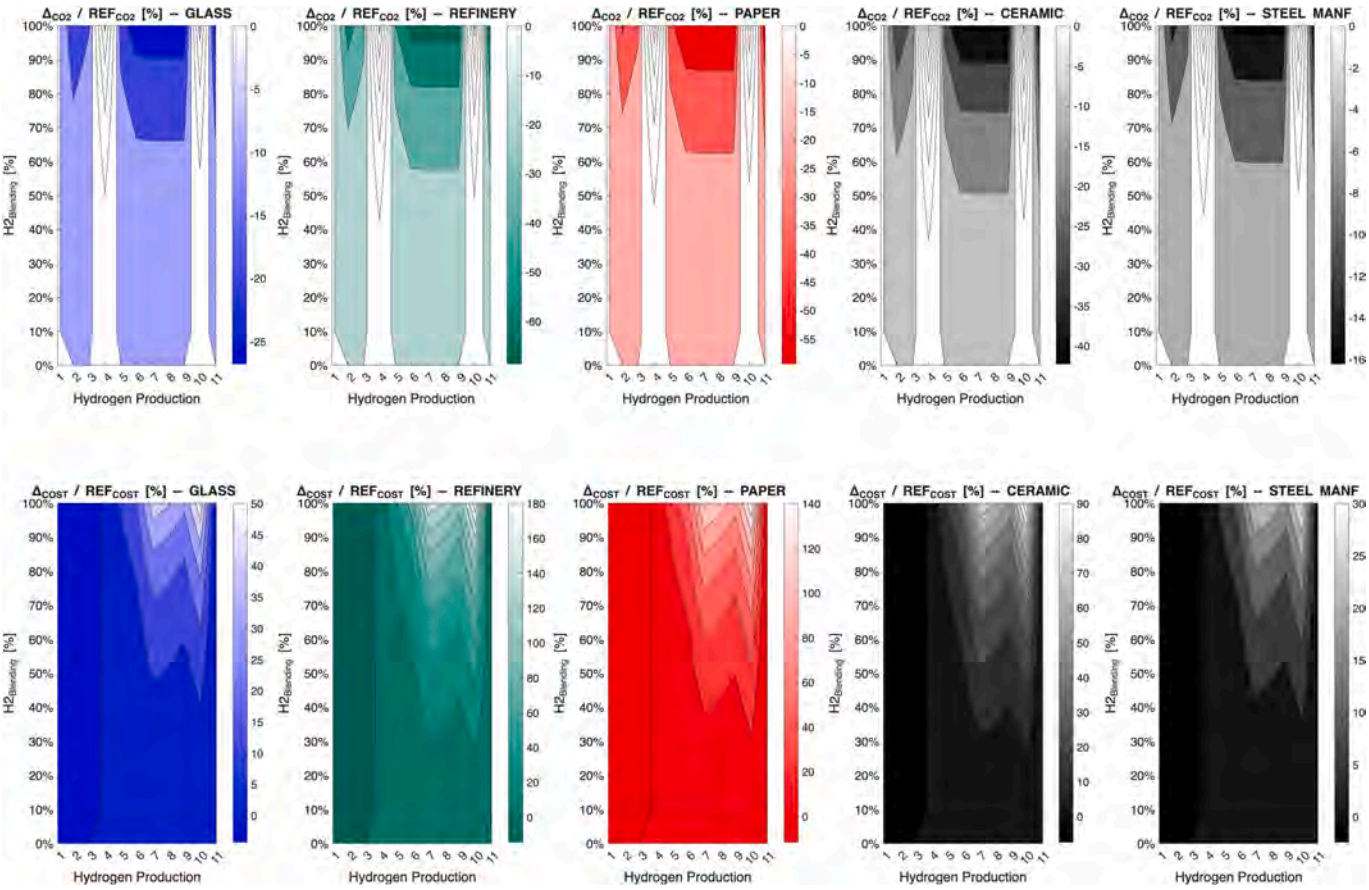

Fig. 13. Potential CO_2 emissions reduction for H2 production type.

percentages indicate a reduction of emissions or costs with respect to the benchmark, while positive values indicate system configuration not effectively convenient, both from an economically perspective neither from an environmental one. In all plots, the white dashed line represents the zero-variation contour and therefore identifies the combinations of H_2 quality and blending level that keep the corresponding indicator at parity with the reference case. Indeed, results in Fig. 12 highlight that the impact of H_2 integration strongly depends on both the H_2 emission factor and the relative weight of thermal demand in each sector (CO_{2H}/CO_{2TOT} from Table 3). In all sectors, moving towards higher H_2 blending and lower H_2 emission factors drives the system into regions with negative ΔCO_2/REF whereas high blends combined with carbon-intensive H_2 rapidly become unfavourable. This behaviour is particularly pronounced for sectors characterised by a high contribution of thermal emissions.

According to the above, the Oil & Gas refinery sector is confirmed as the most affected by H_2 integration, since it shows the highest CO_{2H}/CO_{2TOT} factor among the HTA sectors considered. When 100% of the thermal demand is supplied by low-carbon H_2 (downwards region of the plot), total CO_2 emissions in the refinery sector decrease from about 80 $kgCO_2$/ton in the benchmark case to values of the order of 30 $kgCO_2$/ton, corresponding to a reduction close to 70%.

If, instead, H_2 is produced via high-carbon routes (upper part of the plot), the same blending level can increase total emissions well above the baseline, confirming that not all H_2 is intrinsically "green". Similar trends are observed in the paper and glass sectors, which are also characterised by high CO_{2H}/CO_{2TOT} ratios. In the pulp & paper sector, the deepest reductions (ΔCO_2/REF $\approx -30\%$) are achieved at high blending levels and low H_2 emission factors, while for unfavourable H_2 production routes CO_2 savings remain marginal or can even turn into penalties.

Conversely, when the CO_{2H}/CO_{2TOT} ratio is low and electrical consumption is predominant, the benefit of H_2 blending becomes less relevant. This is clearly visible in the Iron & Steel Manufacturing sector, where even the most favourable H_2 scenarios lead to a reduction in total emissions from about 260 $kgCO_2$/ton to roughly 220 $kgCO_2$/ton, leading to a maximum reduction of up to 15%. In the ceramic sector, absolute emissions are relatively low already in the reference configuration; H_2 integration still produces noticeable percentage reductions in favourable regions of the map, but the absolute mitigation potential is more limited compared to refineries or the paper industry.

Fig. 12 also highlights the corresponding normalised operating costs, where the vertical axis refers to the specific cost of H_2 and the colour scale represents ΔCost/REF. In all sectors, the cost response is monotonic: at a given H_2 quality, increasing the blending ratio systematically increases the total cost, while decreasing the H_2 price shifts the whole surface downwards. The zero-variation line has a positive slope, indicating that low H_2 prices allow for higher blending levels at cost parity, whereas high H_2 prices restrict economically acceptable blends to low values. Looking again at the refinery sector as an example, at low H_2 prices there exists a broad operating region where ΔCost/REF remains close to zero for blending levels up to 30–40%, meaning that significant CO_2 reductions can be achieved at nearly constant OPEX. When the specific cost of H_2 approaches the upper bound of the range, however, the cost increase becomes substantial, with ΔCost/REF exceeding +80% for higher blending ratios. A similar behaviour can be observed in the paper and glass sectors, where the larger thermal demand per tonne of produced good amplifies the cost impact of H_2. In the most extreme cases, the equivalent cost per ton more than doubles with respect to the benchmark. In the ceramic and Iron & Steel Manufacturing sectors, the gradients are milder, reflecting the lower weight of H_2 in the overall energy balance; nevertheless, high H_2 prices coupled with high blending

levels also lead to significant cost penalties.

Looking instead at the H2 production types of Table 4, Fig. 13 summarises the decarbonization potential of the different H_2 production technologies in a more direct way. Indeed, only the system configuration characterized by CO_2 reduction is represented with colours, while for H2 production type characterized by higher than 230 $kgCO_2$/MWh of heat, the CO_2 figures shows white areas. These results confirm that, in the separate production of heat and electricity for HTA sectors, only a restricted set of H_2 production technologies simultaneously allows for substantial CO_2 emission reductions and acceptable operating costs. In particular, the refinery sector, with $CO_{2H}/CO_{2TOT} \approx 2.2$, can benefit from CO_2 reductions approaching 70% when supplied with low-carbon H_2, whereas for sectors with lower thermal shares the maximum achievable reduction is much smaller. Conversely, operating costs increase in almost all configurations, highlighting that additional policy instruments or market mechanisms are required to make deep decarbonization via H_2 blending economically viable.

Given the trend of the results of the Glass and Refinery HTA sectors, the authors have presented for these two sectors a deeper analyses review since are the once characterized by the most prominent decarbonization potential. For doing so, the comparative assessment of the Glass and Refinery sectors is shown in Fig. 14, where normalised variations of CO_2 emissions and operating costs are represented as overlaid three-dimensional surfaces. In both figures, the Glass sector is shown in blue and the Refinery sector in green. The emissions plot indicates a substantially steeper response for refineries: for low-carbon hydrogen (CO_2 factor $<$ 30–40 $kgCO_2$/MWh) and high blending levels ($>$ 80%), refineries achieve CO_2 reductions close to −70%, while glass manufacturing typically reaches between −40% and − 50%. When hydrogen with unfavourable emission factors ($>$ 250 $kgCO_2$/MWh) is used, the refinery surface crosses rapidly into positive region, generating penalties above +40% at full substitution, whereas the glass sector generally remains within a + 10% to +25% range. This contrast reflects the markedly different CO_{2H}/CO_{2TOT} ratios of the two sectors: in refineries, fuel-related emissions dominate the total footprint, so altering the fuel mix produces a proportionally larger effect.

The cost comparison exhibits a similar disparity. At low hydrogen prices ($<$ 50 €/MWh), both sectors remain close to their reference condition for blending ratios up to approximately 40–50%, with ΔCost/REF remaining below +10%. As hydrogen costs rise toward 150–200 €/MWh, refinery costs increase sharply, surpassing +100% at full blending, while the glass sector typically experiences more moderate increases in the +40% to +60% range. This behaviour confirms that refinery economics are significantly more sensitive to both hydrogen price and blending extent due to the higher share of thermal fuel in their operational expenditure. Overall, the two surfaces demonstrate that identical hydrogen pathways and blending strategies yield markedly different normalised impacts across HTA segments. Refineries present a high leverage for decarbonisation capable of deep emission cuts when low-carbon, low-cost hydrogen is available, but also show the largest sensitivity to high hydrogen prices or carbon intensities. The Glass sector, by contrast, shows a more moderate and more resilient response.

The comparative analysis of CO_2 emissions across the five HTA sectors highlights the substantial variability in both baseline emissions and the decarbonisation potential achievable through full fuel switching to hydrogen, to summarize the results, looking at Figs. 15 and 16, it can be observed that when hydrogen is supplied via low-carbon electrolysis powered by nuclear energy, all sectors experience marked reductions in total CO_2 emissions, with refinery operations achieving the most pronounced decline (−68%), followed by paper (−59%), ceramic (−42%), glass (−26%) and steel manufacturing (−16%). Conversely, when hydrogen is produced through carbon-intensive gasification, full substitution of natural gas leads to significant emission penalties in every sector, with increases exceeding +90% for paper and refinery and ranging from +25% to +66% in the remaining sectors. These results emphasise that the effectiveness of hydrogen as a decarbonisation vector is strongly contingent on its upstream carbon intensity, and they further demonstrate that sector-specific characteristics, including baseline thermal demand and process efficiency, critically influence the magnitude of achievable emission reductions.

These findings highlight the necessity of sector-specific policies, pricing mechanisms and hydrogen procurement strategies rather than uniform measures across the HTA domain. The obtained results are aligned with studies found in the most up to date SoA [43,73], highlighting how the proposed methodology for exploring the H2 blending solutions is sounded.

6. Conclusion

The decarbonisation of Hard-to-Abate (HTA) sectors is essential for meeting 2050 climate targets, especially where deep process retrofits remain at low TRL and high cost. In this context, fuel diversification and the progressive integration of hydrogen into energy-intensive industries such as Glass, Iron & Steel, Paper and Refinery offer a near- to medium-term pathway to reduce the carbon intensity of existing assets without structural changes to core processes. To assess the viability of this transition, the authors proposed a methodological approach based on matching HTA sector demands (e.g. electricity, heat) together with

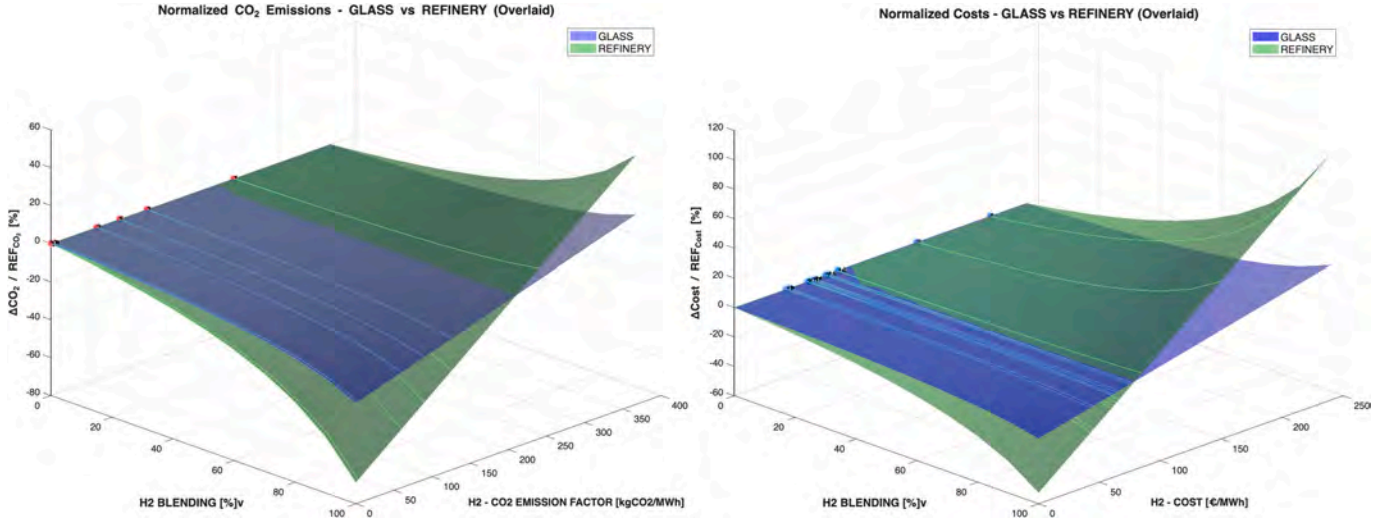

Fig. 14. H2 blending glass vs refinery – normalized emission reduction (left) and costs (right).

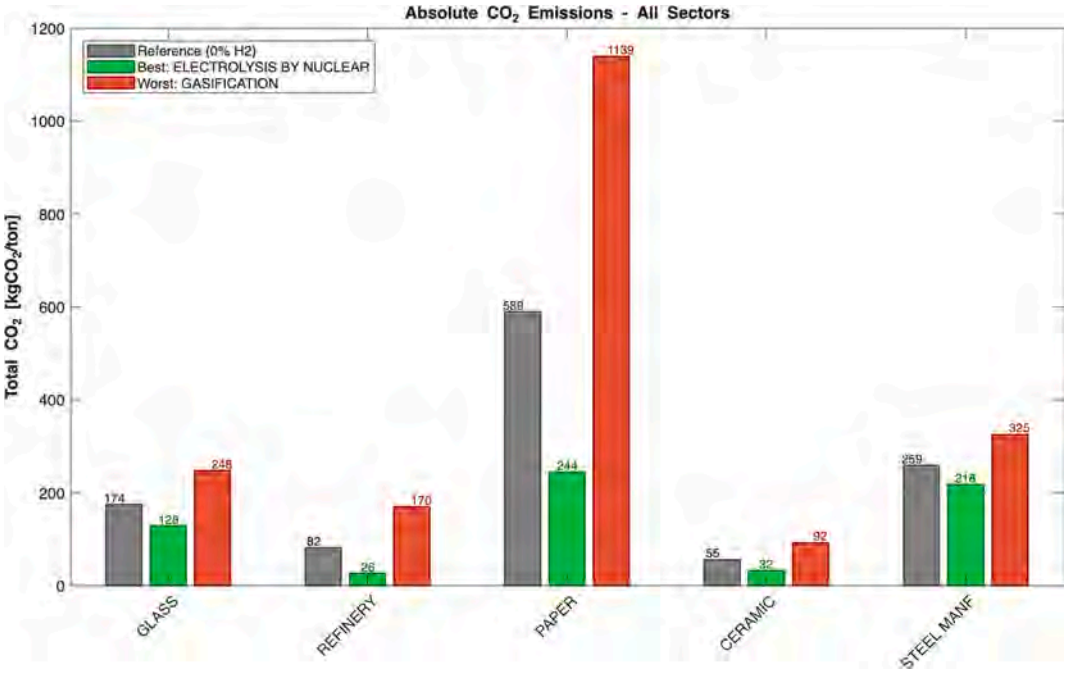

Fig. 15. 100% H2 blending in all HTA sectors vs reference 0% H2 blending (best vs worst case).

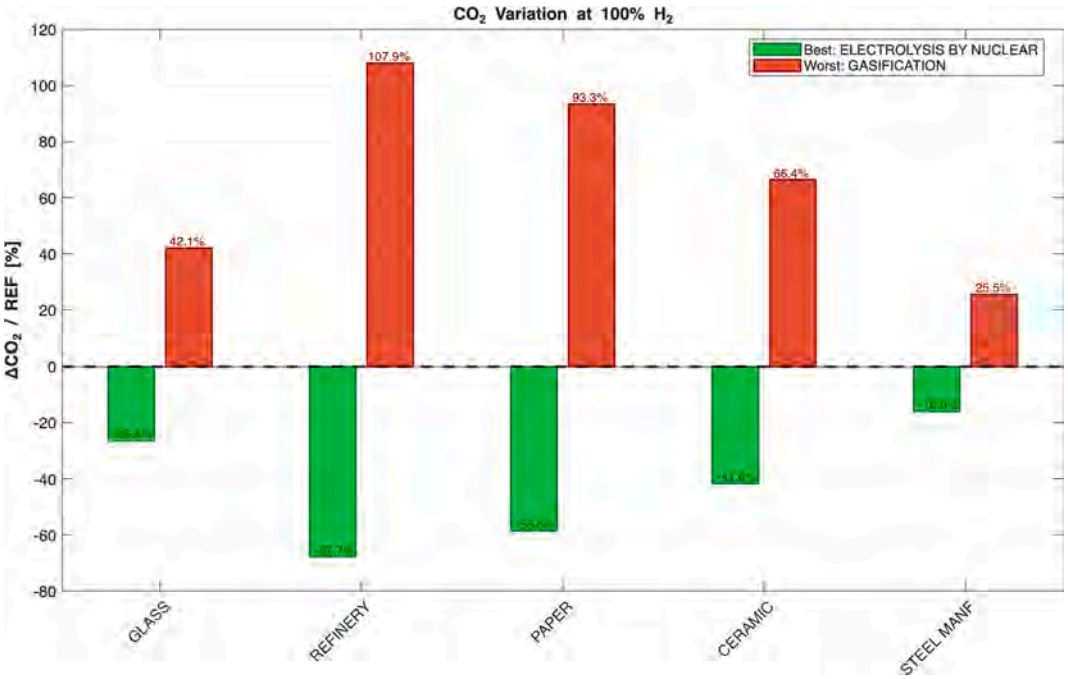

Fig. 16. 100% H2 blending in all HTA sectors - best vs worst case.

multi-energy system generating technologies (e.g. CHP, furnace and, boilers), fed by hydrogen.

On the demand side, an Energy Consumption Model and a dedicated HTA database quantify specific heat and electricity consumption per unit of output and the associated specific CO_2 emissions. On the supply side, an Energy Supply Model incorporates a broad portfolio of hydrogen production routes from coal gasification and SMR to green electrolysis and biomass-based options each characterised by levelized cost of hydrogen (LCOH), specific CO_2 emissions, TRL and synthetic KPIs. This dual-database and fuel-mix optimisation approach fills a gap in the existing literature, which typically addresses individual technologies or single sectors, by providing a general and customisable framework that links hydrogen technology choices to sector-resolved decarbonisation potential and cost impacts.

The proposed methodology is then used when simulating case studies. Indeed, the authors focuses on heat decarbonisation via H_2–CH_4 blending in fuel boilers, delivering a ready-to-be-used approach for understanding blending potential through “maps” that express CO_2 reduction and cost variation as a function of hydrogen emission factor and blending ratio. For example, imposing a 20% reduction target relative to the reference case requires about 70% blending when using blue hydrogen with an emission factor of 80 $kgCO_2$/MWh, whereas only

50% is needed with near-zero-carbon green hydrogen. Under a CH_4 price of 70 €/MWh and a CO_2 tax of 100 €/ton, green hydrogen remains more expensive than the baseline, while blue hydrogen yields a modest OPEX reduction of roughly 2 €/MWh. When these results are projected onto different HTA sectors, refineries, characterised by a CO_2H/CO_2E ratio of about 2.2, can reach Scope 1 CO_2 reductions close to 70%, whereas Iron & Steel Manufacturing, with a lower thermal share, exhibits a maximum reduction potential of around 15%. The cross-sector comparison further shows that low-carbon hydrogen (e.g. nuclear-powered electrolysis) can deliver also Scope 1 CO_2 reductions of −59% for Paper, −42% for Ceramic, −26% for Glass, while hydrogen from gasification can increase emissions by more than +90% in some sectors. These findings highlight both the decisive role of upstream hydrogen carbon intensity and the importance of sector-specific energy structures and that including baseline thermal demand and process efficiency, critically influence the magnitude of achievable emission reductions.

The present work intentionally focuses on heat supplied by gas/H_2 boilers and does not yet include CHP, heat pumps or electric boilers, as a rigorous simulation of combined generation of heat and electricity would require additional detail on temperature levels, mass flow rates and process integration constraints.

The primary aim of the paper is to highlight and present a well-structured, generalisable methodology for addressing HTA sector decarbonisation. Following the same approach, it will be possible to investigate alternative scenarios, not only in terms of technological configuration, by subsequently integrating electricity decarbonisation options such as CHP, electric boilers, heat pumps and low-carbon power mixes, but also in terms of policy design, including incentivisation mechanisms, differentiated CO_2 prices and the explicit trading mechanism of CO_2 credits. In this perspective, the proposed methodology and databases built up by the authors provide a robust and transparent decision-support tool to design sector-specific hydrogen deployment strategies and multi-energy system configurations that are both technically viable and aligned with Paris-compatible transition pathways.

Nomenclature

ABCH	Absorption Chiller
BO	Boiler
C	Cold Energy
CCGT	Combined Cycle Gas Turbine
CP	Cooling Power
Cp	Capacity Production
CHP	Combined Heat & Power
COP	Coefficient of Performance
DB	Database
E	Electricity
f_{CO2}	CO_2 Specific Emission Factor
F	Fuel
GT	Gas Turbine
H	Heat
HT	High Temperature
HTA	Hard to Abate
HP	Heat Pump
ICE	Internal Combustion Engine
LCOH	Levelized Cost of Hydrogen
LHV	Low Heating Value
LT	Low Temperature
m	mass flow rate
MT	Medium Temperature
j, k, N	Cardinal Number
P	Power
PM	Molecular Weigh
PP	Power Plant
Q	Heat Power
RES	Renewable Energy Source
RO	Reverse Osmosis
SSBT	Steam Cycle Back-Pressure Turbine
SSCT	Steam Cycle Condensing Turbine
T	Temperature
t	time
VCCH	Vapour Compression Chiller
W	Water

Greek symbols

η	efficiency
$\in$	specific cost

Sup/subscripts

+/−	Imported/Exported
0	Specific CAPEX
BL	Blend
D	Demand
G	Grid
J	j-th element
R	Reference
S	Supply
SC	Specific Consumption
TOT	Total

CRediT authorship contribution statement

S. Mazzoni: Writing – original draft, Visualization, Validation, Software, Methodology, Investigation, Formal analysis, Data curation, Conceptualization. **M. Vellini:** Writing – review & editing, Visualization, Supervision, Data curation. **M. Gambini:** Writing – review & editing, Supervision.

Declaration of competing interest

The authors declare that they have no known competing financial interests or personal relationships that could have appeared to influence the work reported in this paper.

Data availability

Data will be made available on request.

References

[1] https://unfccc.int/topics/global-stocktake. n.d.
[2] https://unfccc.int/news/cop28-agreement-signals-beginning-of-the-end-of-the-fossil-fuel-era. n.d.
[3] Final report of the high-level panel of the european decarbonisation pathways initiative n.d. Doi: https://doi.org/10.2777/476014.
[4] Gailani A, Cooper S, Allen S, Pimm A, Taylor P, Gross R. Assessing the potential of decarbonization options for industrial sectors. Joule 2024;8:576–603. https://doi.org/10.1016/j.joule.2024.01.007.
[5] Scheffler F, Imdahl C, Zellmer S, Herrmann C. Techno-economic and environmental assessment of renewable hydrogen import routes from overseas in 2030. Appl Energy 2025:380. https://doi.org/10.1016/j.apenergy.2024.125073.
[6] https://www.iea.org/reports/energy-technology-perspectives-2020. n.d.
[7] Mitigating greenhouse gas emissions in Hard-to-Abate sectors. 2022.
[8] Kawai E, Ozawa A, Matsuhasi R. Techno-economic analysis with a dynamic optimization approach integrating electrical and chemical engineering: a case study for aviation decarbonization in Japan. Appl Energy 2026;402:126966. https://doi.org/10.1016/j.apenergy.2025.126966.
[9] Energy Agency I. Iron and steel technology roadmap towards more sustainable steelmaking part of the energy technology perspectives series. n.d.
[10] Wang RR, Zhao YQ, Babich A, Senk D, Fan XY. Hydrogen direct reduction (H-DR) in steel industry—an overview of challenges and opportunities. J Clean Prod 2021:329. https://doi.org/10.1016/j.jclepro.2021.129797.
[11] Keys A, Van Hout M, Daniëls B. Decarbonisation options for the Dutch steel industry manufacturing industry decarbonisation data exchange network decarbonisation options for the Dutch steel industry. 2019.
[12] The use of hydrogen in the iron and steel industry. 2018.

[13] Kazmi B, Taqvi SAA, Juchelková D. State-of-the-art review on the steel decarbonization technologies based on process system engineering perspective. Fuel 2023:347. https://doi.org/10.1016/j.fuel.2023.128459.
[14] Ren M, Lu P, Liu X, Hossain MS, Fang Y, Hanaoka T, et al. Decarbonizing China's iron and steel industry from the supply and demand sides for carbon neutrality. Appl Energy 2021:298. https://doi.org/10.1016/j.apenergy.2021.117209.
[15] hsbc-transition-pathways-industrials-and-chemicals-key-findings n.d.
[16] https://www.missionpossiblepartnership.org/wp-content/uploads/2022/09/Making-1.5-Aligned-Ammonia-possible.pdf. n.d.
[17] Eerens H, Van Dam D. Decarbonisation options for large volume organic chemicals production, DOW chemical Terneuzen manufacturing industry decarbonisation data exchange network colophon decarbonisation options for large volume organic chemicals production, DOW terneuzen. 2022.
[18] Cai B, Wang J, He J, Geng Y. Evaluating CO2 emission performance in China's cement industry: an enterprise perspective. Appl Energy 2016;166:191–200. https://doi.org/10.1016/j.apenergy.2015.11.006.
[19] CEMCAP Action full title: CO2 capture from cement production type of action: D4.6 CEMCAP comparative techno-economic analysis of CO2 capture in cement plants. 2015.
[20] Energy consumption benchmark guide: Cement clinker production natural resources Canada ressources naturelles Canada. n.d.
[21] Schneider M, Romer M, Tschudin M, Bolio H. Sustainable cement production-present and future. Cem Concr Res 2011;41:642–50. https://doi.org/10.1016/j.cemconres.2011.03.019.
[22] Benchmarking report for the cement sector. In: Industrial energy efficiency project; 2014.
[23] The view of cement sector powering the cement industry. n.d.
[24] Song D, Yang J, Chen B, Hayat T, Alsaedi A. Life-cycle environmental impact analysis of a typical cement production chain. Appl Energy 2016;164:916–23. https://doi.org/10.1016/j.apenergy.2015.09.003.
[25] Raffetti E, Treccani M, Donato F. Cement plant emissions and health effects in the general population: a systematic review. Chemosphere 2019;218:211–22. https://doi.org/10.1016/j.chemosphere.2018.11.088.
[26] Williams F, Yang A, Nhuchhen DR. Decarbonisation pathways of the cement production process via hydrogen and oxy-combustion. Energ Conver Manage 2024:300. https://doi.org/10.1016/j.enconman.2023.117931.
[27] https://www.missionpossiblepartnership.org/wp-content/uploads/2021/12/Closing-the-Gap-for-Aluminium-Emissions.pdf n.d.
[28] Gerbens-Leenes PW, Hoekstra AY, Bosman R. The blue and grey water footprint of construction materials: Steel, cement and glass. Water Resour Ind 2018;19:1–12. https://doi.org/10.1016/j.wri.2017.11.002.
[29] Serge Roudier, Maria Scalet B, Marcos Garcia Muñoz, Luis Delgado Sancho, Querol Sissa A. Best available techniques (BAT) reference document for the manufacture of glass : Industrial emissions Directive 2010/75/EU: Integrated pollution prevention and control. Publications Office; 2013.
[30] Zier M, Stenzel P, Kotzur L, Stolten D. A review of decarbonization options for the glass industry. Energy Convers Manag 2021:10. https://doi.org/10.1016/j.ecmx.2021.100083.
[31] Atzori D, Bassano C, Rossi E, Tiozzo S, Corasaniti S, Spena A. Hydrogen cost and carbon analysis in hollow glass manufacturing. Energies (Basel) 2025:18. https://doi.org/10.3390/en18154105.
[32] Leefomgeving;TNO P Manufacturing industry decarbonisation data exchange network (MIDDEN) - The database Https://PolicycommonsNet/Artifacts/1978761/Manufacturing-Industry-Decarbonisation-Data-Exchange-Network-Midden/2730526/; 2021.
[33] Griffiths S, Sovacool BK, Kim J, Bazilian M, Uratani JM. Decarbonizing the oil refining industry: a systematic review of sociotechnical systems, technological innovations, and policy options. Energy Res Soc Sci 2022:89. https://doi.org/10.1016/j.erss.2022.102542.
[34] Jing L, El-Houjeiri HM, Monfort JC, Brandt AR, Masnadi MS, Gordon D, et al. Carbon intensity of global crude oil refining and mitigation potential. Nat Clim Chang 2020;10:526–32. https://doi.org/10.1038/s41558-020-0775-3.
[35] Ibn-Mohammed T, Randall CA, Mustapha KB, Guo J, Walker J, Berbano S, et al. Decarbonising ceramic manufacturing: a techno-economic analysis of energy efficient sintering technologies in the functional materials sector. J Eur Ceram Soc 2019;39:5213–35. https://doi.org/10.1016/j.jeurceramsoc.2019.08.011.
[36] Bechara CA, Alnouri SY. Energy assessment strategies in carbon-constrained industrial clusters. Energ Conver Manage 2022:254. https://doi.org/10.1016/j.enconman.2021.115204.
[37] Bekele EA, Sgaramella A, Ciancio A, Lo Basso G, de Santoli L, Pastore LM. Hydrogen valleys to foster local decarbonisation targets: a multiobjective optimisation approach for energy planning. Appl Energy 2025:402. https://doi.org/10.1016/j.apenergy.2025.126851.
[38] Gambini M, Vellini M. On selection and optimal design of cogeneration units in the industrial sector. J Sustain Dev Energy Water Environ Syst 2019;7:168–92. https://doi.org/10.13044/j.sdewes.d6.0236.
[39] Vellini M, Gambini M, Stilo T. High-efficiency cogeneration systems for the food industry. J Clean Prod 2020:260. https://doi.org/10.1016/j.jclepro.2020.121133.
[40] Gambini M, Vellini M, Stilo T, Manno M, Bellocchi S. High-efficiency cogeneration systems: the case of the paper industry in Italy. Energies (Basel) 2019:12. https://doi.org/10.3390/en12030335.
[41] Raillard-Cazanove Q, Rogeau A, Girard R. Decarbonisation modelling for key industrial sectors focusing on process changes in a cost-optimised pathway. Appl Energy 2025:382. https://doi.org/10.1016/j.apenergy.2024.125206.
[42] Mazzoni S, Ooi S, Nastasi B, Romagnoli A. Energy storage technologies as techno-economic parameters for master-planning and optimal dispatch in smart multi energy systems. Appl Energy 2019;254:113682. https://doi.org/10.1016/j.apenergy.2019.113682.
[43] Lo Basso G, Pastore LM, Sgaramella A, Mojtahed A, Ciancio A, Massulli AR, et al. Status and perspectives of hydrogen role for decarbonising industry: a comprehensive review. Renew Sustain Energy Rev 2025:224. https://doi.org/10.1016/j.rser.2025.116083.
[44] Gambini M, Mazzoni S, Vellini M. The role of cogeneration in the electrification pathways towards decarbonization. Energies (Basel) 2023;16. https://doi.org/10.3390/en16155606.
[45] Osman AI, Mehta N, Elgarahy AM, Hefny M, Al-Hinai A, Al-Muhtaseb AH, et al. Hydrogen production, storage, utilisation and environmental impacts: a review. Environ Chem Lett 2022;20:153–88. https://doi.org/10.1007/s10311-021-01322-8.
[46] Nikolaidis P, Poullikkas A. A comparative overview of hydrogen production processes. Renew Sustain Energy Rev 2017;67:597–611. https://doi.org/10.1016/j.rser.2016.09.044.
[47] Pinsky R, Sabharwall P, Hartvigsen J, O'Brien J. Comparative review of hydrogen production technologies for nuclear hybrid energy systems. Prog Nuclear Energy 2020:123. https://doi.org/10.1016/j.pnucene.2020.103317.
[48] https://aenert.com/news-events/energy-news-monitoring/n/direct-conversion-of-methane-to-hydrogen-by-pyrolysis-status-and-prospects/. n.d.
[49] Rawat S, Rautela A, Yadav I, Misra S, Kumar S. A comprehensive review on enhanced biohydrogen production: pretreatment, applied strategies, techno-economic assessment, and future perspective. Bioenergy Res 2023;16:2131–54. https://doi.org/10.1007/s12155-023-10598-3.
[50] Tavares Borges P, Silva Lora EE, Venturini OJ, Errera MR, Yepes Maya DM, Makarfi Isa Y, et al. A comprehensive technical, environmental, economic, and bibliometric assessment of hydrogen production through biomass gasification, including global and brazilian potentials. Sustainability (Switzerland) 2024;16. https://doi.org/10.3390/su16219213.
[51] Vu H, Chang D. Life cycle global warming impact of a green hydrogen supply chain: a case study of Australia to South Korea. Appl Energy 2025:397. https://doi.org/10.1016/j.apenergy.2025.126339.
[52] Hydrogen-based power generation II. A net-zero backup solution for green ammonia hubs table of content 1.1 Global hydrogen outlook 5 1.2 Technologies for hydrogen transportation 6. n.d.
[53] Hydrogen-powered gensets for electric vehicle charging. n.d.
[54] Xiang P, Jiang K, Wang J, He C, Chen S, Jiang W. Evaluation of LCOH of conventional technology, energy storage coupled solar PV electrolysis, and HTGR in China. Appl Energy 2024:353. https://doi.org/10.1016/j.apenergy.2023.122086.
[55] Deloitte. Green hydrogen: Energizing the path to net zero. n.d.
[56] Mazzoni S, Nastasi B, Ooi S, Desideri U, Comodi G, Romagnoli A. The adoption of a planning tool software platform for optimized polygeneration design and operation – a district cooling application in South-East Asia. Appl Therm Eng 2021:199. https://doi.org/10.1016/j.applthermaleng.2021.117532.
[57] Simeoni P, Nardin G, Ciotti G. Planning and design of sustainable smart multi energy systems. The case of a food industrial district in Italy. Energy 2018;163:443–56. https://doi.org/10.1016/j.energy.2018.08.125.
[58] Bühler F, Petrović S, Karlsson K, Elmegaard B. Industrial excess heat for district heating in Denmark. Appl Energy 2017;205:991–1001. https://doi.org/10.1016/j.apenergy.2017.08.032.
[59] Liew PY, Walmsley TG, Wan Alwi SR, Abdul Manan Z, Klemeš JJ, Varbanov PS. Integrating district cooling systems in locally integrated energy sectors through total site heat integration. Appl Energy 2016;184:1350–63. https://doi.org/10.1016/j.apenergy.2016.05.078.
[60] Hosseinian SM, Nezamoleslami R. Water footprint and virtual water assessment in cement industry: a case study in Iran. J Clean Prod 2016;172:2454–63. https://doi.org/10.1016/j.jclepro.2017.11.164.
[61] Sun P, Elgowainy A, Wang M, Han J, Henderson RJ. Estimation of U.S. refinery water consumption and allocation to refinery products. Fuel 2018;221:542–57. https://doi.org/10.1016/j.fuel.2017.07.089.
[62] Cantini A, Leoni L, Ferraro S, De Carlo F, Martini C, Martini F, et al. Technological energy efficiency improvements in glass-production industries and their future perspectives in Italy. Processes 2022:10. https://doi.org/10.3390/pr10122653.
[63] Daniarta S, Błasiak P, Kolasiński P, Imre AR. Sustainability by means of cold energy utilisation-to-power conversion: a review. Renew Sustain Energy Rev 2024:205. https://doi.org/10.1016/j.rser.2024.114833.
[64] Wang Y, Zhang H, Ji S, Frate GF, Duan L, Desideri U, et al. Techno-economic analysis of a novel heat-power decoupling system of molten salt coupled steam accumulator used in gas-steam combined cycle CHP unit. Appl Energy 2025:400. https://doi.org/10.1016/j.apenergy.2025.126591.
[65] Gambini M, Vellini M. High efficiency cogeneration: electricity from cogeneration in CHP plants. In: Energy Procedia. 81. Elsevier Ltd; 2015. p. 430–9. https://doi.org/10.1016/j.egypro.2015.12.117.
[66] Pohl C, Schüler G, Schiereck D. Borrower- and lender-specific determinants in the pricing of sustainability-linked loans. J Clean Prod 2023:385. https://doi.org/10.1016/j.jclepro.2022.135652.
[67] Artiga Gonzalez T, Capera Romero L, Karmaziene E, Yuan X. Green gains: the impact of REITs' environmental performance on sustainability-linked loan interest rates. Financ Res Lett 2025:71. https://doi.org/10.1016/j.frl.2024.106415.
[68] Daurer G, Schwarz S, Demuth M, Gaber C, Hochenauer C. Experimental and numerical analysis of industrial-type low-swirl combustion of hydrogen enriched natural gas including OH* chemiluminescence imaging. Int J Hydrogen Energy 2024;80:890–906. https://doi.org/10.1016/j.ijhydene.2024.07.119.

[69] Zhang J, Clennell MB, Chen Y. New analytical thermodynamic models developed for pure H2, CH4, CO2 and H2 containing mixtures based on molecular simulations. Int J Hydrogen Energy 2024;69:687–97. https://doi.org/10.1016/j.ijhydene.2024.05.097.
[70] ISPRA. Edition 2024 efficiency and decarbonization indicators in Italy and in the biggest European countries. 2024.
[71] Terna Dati statistici sull'energia elettrica in Italia - 2023, https://download.terna.it/terna/ANNUARIO%20STATISTICO%202023_8dd1f6457916183.pdf.
[72] Arera, Relazione Annuale 2022, Stato dei Servizi -Volume 1.
[73] Oluleye G, McLaughlin S, Steen E, Wu S, Hanna R, Heptonstall P. Blending interventions to achieve green hydrogen cost competitiveness for industrial decarbonisation. Int J Hydrogen Energy 2025;144:1343–57. https://doi.org/10.1016/j.ijhydene.2025.03.420.